

**Off-line and
On-line
Applications**

**of High Resolution
Laser Spectroscopy
on Exotic Species**

—

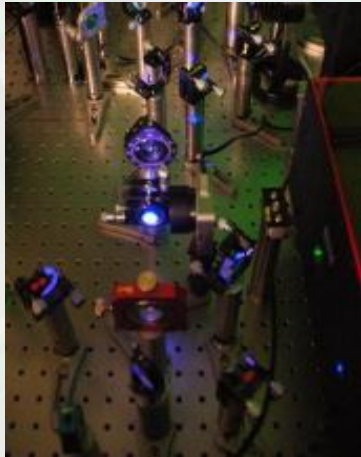
Collinear and Alternative Approaches

Klaus D.A. Wendt

Institut für Physik, Johannes Gutenberg-Universität Mainz

Outline

- **The Study of Exotic Nuclides** – from the Periodic Table to the Nuclear Chart
- **Scientific Findings and Data** from laser spectroscopy



- experimental prerequisites and techniques
- high resolution laser spectroscopy
- line broadenings
- collinear versus other experimental techniques



- **Some Specific Results** on most **Exotic Elements** and **Isotopes**
- **Summary and Outlook**

The Periodic System 2019 – with today's Exotic Elements

PERIODIC TABLE Atomic Properties of the Elements

Definition of Exotic Elements:

abundance in the geosphere

$\ll 10^{-9}$ ppm (10^{-15})

^{43}Tc , ^{61}Pm , ^{85}At , ^{87}Fr , Acti- & Transactinides

For the most accurate values of these and other constants, visit ml.nist.gov/constants.

☐ Solids
☐ Liquids
☐ Gases
☐ Artificially Prepared

NIST National Institute of Standards and Technology
U.S. Department of Commerce

Physical Measurement Laboratory www.nist.gov/pml
Standard Reference Data www.nist.gov/srd

Atomic Properties of the Elements

NIST National Institute of Standards and Technology
U.S. Department of Commerce

Physical Measurement Laboratory www.nist.gov/pml
Standard Reference Data www.nist.gov/srd

Definition of Exotic Elements:

abundance in the geosphere

$\ll 10^{-9}$ ppm (10^{-15})

^{43}Tc , ^{61}Pm , ^{85}At , ^{87}Fr , Acti- & Transactinides

For the most accurate values of these and other constants, visit ml.nist.gov/constants.

Legend:
Solid
Liquid
Gas
Artificially Prepared

Period

Group	1	2	3	4	5	6	7	8	9	10	11	12	13	14	15	16	17	18
IA	IIA	IIIA	IVA	VA	VIA	VIIA	VIIIA	VIIIA	VIIIA	VIIIA	IB	IIB	IIIA	IVA	VA	VIA	VIIA	VIIIA
1	H Hydrogen 1.008 $1s$ 13.5984																	He Helium 4.0026 $1s^2$ 24.5874
2	Li Lithium 6.94 $1s^2 2s$ 5.3917	Be Beryllium 9.0122 $1s^2 2s^2$ 9.3227											B Boron 10.81 $1s^2 2s^2 2p$ 8.2880	C Carbon 12.011 $1s^2 2s^2 2p^2$ 11.2603	N Nitrogen 14.007 $1s^2 2s^2 2p^3$ 14.5341	O Oxygen 15.999 $1s^2 2s^2 2p^4$ 13.6181	F Fluorine 18.998 $1s^2 2s^2 2p^5$ 17.4228	Ne Neon 20.180 $1s^2 2s^2 2p^6$ 21.5645
3	Na Sodium 22.990 $[Ne]3s$ 5.1391	Mg Magnesium 24.305 $[Ne]3s^2$ 7.6462											Al Aluminum 26.982 $[Ne]3s^2 3p$ 8.1517	Si Silicon 28.085 $[Ne]3s^2 3p^2$ 8.1517	P Phosphorus 30.974 $[Ne]3s^2 3p^3$ 10.4867	S Sulfur 32.06 $[Ne]3s^2 3p^4$ 10.3600	Cl Chlorine 35.45 $[Ne]3s^2 3p^5$ 12.9876	Ar Argon 39.948 $[Ne]3s^2 3p^6$ 15.7596
4	K Potassium 39.098 $[Ar]4s$ 4.3407	Ca Calcium 40.078 $[Ar]4s^2$ 6.1132	Sc Scandium 44.956 $[Ar]3d^1 4s^2$ 6.5615	Ti Titanium 47.887 $[Ar]3d^2 4s^2$ 6.8281	V Vanadium 50.942 $[Ar]3d^3 4s^2$ 6.7462	Cr Chromium 51.996 $[Ar]3d^5 4s^1$ 6.7665	Mn Manganese 54.938 $[Ar]3d^5 4s^2$ 7.434	Fe Iron 55.845 $[Ar]3d^6 4s^2$ 7.9025	Co Cobalt 58.933 $[Ar]3d^7 4s^2$ 7.8810	Ni Nickel 58.693 $[Ar]3d^8 4s^2$ 7.6399	Cu Copper 63.546 $[Ar]3d^{10} 4s^1$ 7.7264	Zn Zinc 65.38 $[Ar]3d^{10} 4s^2$ 9.3942	Ga Gallium 69.723 $[Ar]3d^{10} 4s^2 4p$ 5.9903	Ge Germanium 72.630 $[Ar]3d^{10} 4s^2 4p^2$ 7.8904	As Arsenic 74.922 $[Ar]3d^{10} 4s^2 4p^3$ 9.7886	Se Selenium 78.971 $[Ar]3d^{10} 4s^2 4p^4$ 9.7524	Br Bromine 79.904 $[Ar]3d^{10} 4s^2 4p^5$ 11.8138	Kr Krypton 83.798 $[Ar]3d^{10} 4s^2 4p^6$ 13.9906
5	Rb Rubidium 85.468 $[Kr]5s$ 4.1771	Sr Strontium 87.62 $[Kr]5s^2$ 5.6949	Y Yttrium 88.906 $[Kr]4d^1 5s^2$ 6.2173	Zr Zirconium 91.224 $[Kr]4d^2 5s^2$ 6.8341	Nb Niobium 92.906 $[Kr]4d^4 5s$ 6.7589	Mo Molybdenum 95.95 $[Kr]4d^5 5s$ 7.0924	Tc Technetium (98) $[Kr]4d^5 5s$ 7.1194	Ru Ruthenium 101.07 $[Kr]4d^7 5s$ 7.3805	Rh Rhodium 102.91 $[Kr]4d^8 5s$ 7.4589	Pd Palladium 106.42 $[Kr]4d^{10}$ 8.3369	Ag Silver 107.87 $[Kr]4d^{10} 5s$ 7.5782	Cd Cadmium 112.41 $[Kr]4d^{10} 5s^2$ 8.9038	In Indium 114.82 $[Kr]4d^{10} 5s^2 5p$ 5.7884	Sn Tin 118.71 $[Kr]4d^{10} 5s^2 5p^2$ 7.3439	Sb Antimony 121.76 $[Kr]4d^{10} 5s^2 5p^3$ 8.6084	Te Tellurium 127.60 $[Kr]4d^{10} 5s^2 5p^4$ 9.0097	I Iodine 126.90 $[Kr]4d^{10} 5s^2 5p^5$ 10.4513	Xe Xenon 131.29 $[Kr]4d^{10} 5s^2 5p^6$ 12.1298
6	Cs Cesium 132.91 $[Xe]6s$ 3.8939	Ba Barium 137.33 $[Xe]6s^2$ 5.2117		Hf Hafnium 178.49 $[Xe]4f^{14} 5d^2 6s^2$ 6.8251	Ta Tantalum 180.95 $[Xe]4f^{14} 5d^3 6s^2$ 7.5499	W Tungsten 183.84 $[Xe]4f^{14} 5d^4 6s^2$ 7.8940	Re Rhenium 186.21 $[Xe]4f^{14} 5d^5 6s^2$ 7.8335	Os Osmium 190.23 $[Xe]4f^{14} 5d^6 6s^2$ 8.4382	Ir Iridium 192.22 $[Xe]4f^{14} 5d^7 6s^2$ 8.9670	Pt Platinum 195.08 $[Xe]4f^{14} 5d^9 6s$ 8.9588	Au Gold 196.97 $[Xe]4f^{14} 5d^{10} 6s$ 9.2256	Hg Mercury 200.59 $[Xe]4f^{14} 5d^{10} 6s^2$ 10.4375	Tl Thallium 204.38 $[Hg]6p$ 6.1083	Pb Lead 207.2 $[Hg]6p^2$ 7.4167	Bi Bismuth 208.98 $[Hg]6p^3$ 7.2855	Po Polonium (209) $[Hg]6p^4$ 8.414	At Astatine (210) $[Hg]6p^5$ 9.3175	Rn Radon (222) $[Hg]6p^6$ 10.7485
7	Fr Francium (223) $[Rn]7s$ 4.0727	Ra Radium (226) $[Rn]7s^2$ 5.2784		Rf Rutherfordium (261) $[Rn]5f^{14} 6d^2 7s^2$ 6.02	Db Dubnium (268) $[Rn]5f^{14} 6d^3 7s^2$ 6.8	Sg Seaborgium (266) $[Rn]5f^{14} 6d^4 7s^2$ 7.8	Bh Bohrium (270) $[Rn]5f^{14} 6d^5 7s^2$ 7.7	Hs Hassium (277) $[Rn]5f^{14} 6d^6 7s^2$ 7.6	Mt Meitnerium (278) $[Rn]5f^{14} 6d^7 7s^2$ 7.6	Ds Darmstadtium (281) $[Rn]5f^{14} 6d^8 7s^2$ 7.6	Rg Roentgenium (282) $[Rn]5f^{14} 6d^9 7s^2$ 7.6	Cn Copernicium (285) $[Rn]5f^{14} 6d^{10} 7s^2$ 7.6	Nh Nihonium (286) $[Rn]5f^{14} 6d^{10} 7s^2 7p$ 7.6	Fl Flerovium (289) $[Rn]5f^{14} 6d^{10} 7s^2 7p^2$ 7.6	Mc Moscovium (289) $[Rn]5f^{14} 6d^{10} 7s^2 7p^3$ 7.6	Lv Livermorium (293) $[Rn]5f^{14} 6d^{10} 7s^2 7p^4$ 7.6	Ts Tennessine (294) $[Rn]5f^{14} 6d^{10} 7s^2 7p^5$ 7.6	Og Oganesson (294) $[Rn]5f^{14} 6d^{10} 7s^2 7p^6$ 7.6
			La Lanthanum 138.91 $[Xe]5d^1 6s^2$ 5.5789	Ce Cerium 140.12 $[Xe]4f^1 5d^1 6s^2$ 5.5386	Pr Praseodymium 140.91 $[Xe]4f^3 6s^2$ 5.4702	Nd Neodymium 144.24 $[Xe]4f^4 6s^2$ 5.5250	Pm Promethium (145) $[Xe]4f^5 6s^2$ 5.577	Sm Samarium 150.36 $[Xe]4f^6 6s^2$ 5.6437	Eu Europium 151.96 $[Xe]4f^7 6s^2$ 5.6794	Gd Gadolinium 157.25 $[Xe]4f^7 5d^1 6s^2$ 6.1498	Tb Terbium 158.93 $[Xe]4f^9 6s^2$ 6.9838	Dy Dysprosium 162.50 $[Xe]4f^{10} 6s^2$ 6.9991	Ho Holmium 164.93 $[Xe]4f^{11} 6s^2$ 6.9946	Er Erbium 167.26 $[Xe]4f^{12} 6s^2$ 6.1077	Tm Thulium 168.93 $[Xe]4f^{13} 6s^2$ 6.1843	Yb Ytterbium 173.05 $[Xe]4f^{14} 6s^2$ 6.2542	Lu Lutetium 174.97 $[Xe]4f^{14} 5d^1 6s^2$ 5.4299	
			Ac Actinium (227) $[Rn]6d^1 7s^2$ 5.3802	Th Thorium (232) $[Rn]6d^2 7s^2$ 6.3067	Pa Protactinium (231) $[Rn]5f^2 6d^1 7s^2$ 5.69	U Uranium 238.03 $[Rn]5f^3 6d^1 7s^2$ 6.1641	Np Neptunium (237) $[Rn]5f^4 6d^1 7s^2$ 6.2655	Pu Plutonium (244) $[Rn]5f^6 7s^2$ 6.1259	Am Americium (243) $[Rn]5f^7 7s^2$ 6.338	Cm Curium (247) $[Rn]5f^8 7s^2$ 5.9914	Bk Berkelium (247) $[Rn]5f^9 7s^2$ 6.1979	Cf Californium (251) $[Rn]5f^{10} 7s^2$ 6.2817	Es Einsteinium (252) $[Rn]5f^{11} 7s^2$ 6.3676	Fm Fermium (257) $[Rn]5f^{12} 7s^2$ 6.5	Md Mendelevium (258) $[Rn]5f^{13} 7s^2$ 6.59	No Nobelium (259) $[Rn]5f^{14} 7s^2$ 6.6	Lr Lawrencium (260) $[Rn]5f^{14} 7s^2 7p^1$ 4.9	

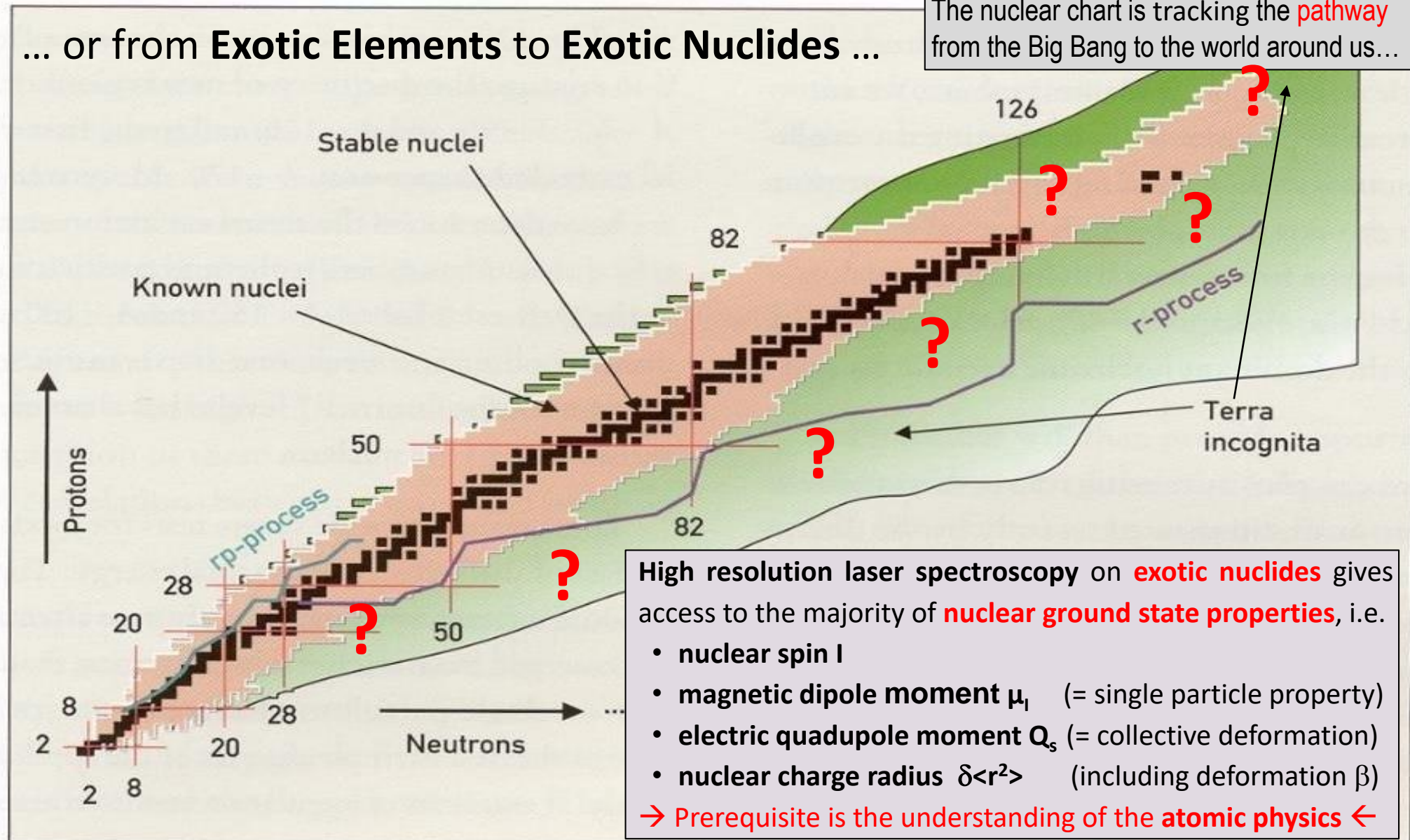
¹Based upon ^{12}C . () indicates the mass number of the longest-lived

...going on-line – heading for exotic isotopes far off stability...

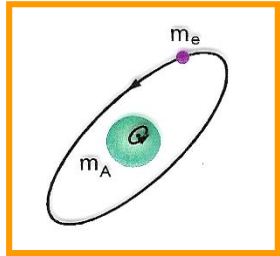
From the Periodic System to the Nuclear Chart...

... or from **Exotic Elements** to **Exotic Nuclides** ...

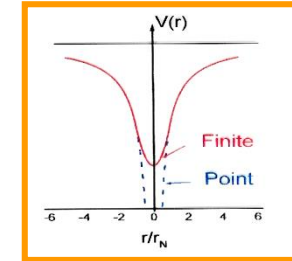
The nuclear chart is tracking the **pathway** from the Big Bang to the world around us...



The Influence of the Nucleus on the Atomic Structure

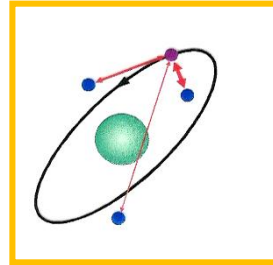


$$H\Psi = E\Psi$$



$$\sum_{i=1}^N \frac{-\hbar^2}{2m} \nabla^2 \quad \leftarrow \quad U+V \quad \rightarrow \quad V(\vec{r}_1\vec{s}_1, \vec{r}_2\vec{s}_2 \dots \vec{r}_n\vec{s}_n)$$

$$\frac{\vec{p}^2}{2\mu} = \sum \frac{\vec{p}_i^2}{2\mu} + \sum_i \sum_{j>i} \frac{\vec{p}_i \cdot \vec{p}_j}{\mu}$$



$$V_{Ze} + \underbrace{V_{Is} + V_{Il}}_{\text{Field Shift}} + \underbrace{V_{ee} + V_{sl} + V_{ss} + V_{ll}}_{\text{pure electronic}}$$

Normal Mass Shift

Specific Mass Shift

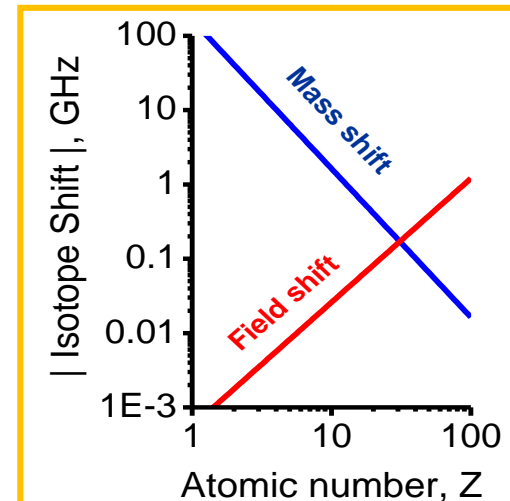
Field Shift

Hyperfine Structure

$$\Delta v_{ij}^{A,A'} = v_{ij}^0 \frac{m_e}{m_p} \frac{(A-A')}{AA'} + C_{ij} v_{ij}^0 \frac{(A-A')}{AA'} + \frac{\pi a_0^3}{Z} \Delta |\Psi(0)|^2 f(Z) [\delta \langle r^2 \rangle^{AA'} + C_l \delta \langle r^4 \rangle^{AA'} + \dots]$$

$$\Delta v_{IS} = (M_N + M_S) \frac{(A-A')}{AA'} + F \delta \langle r^2 \rangle^{AA'}$$

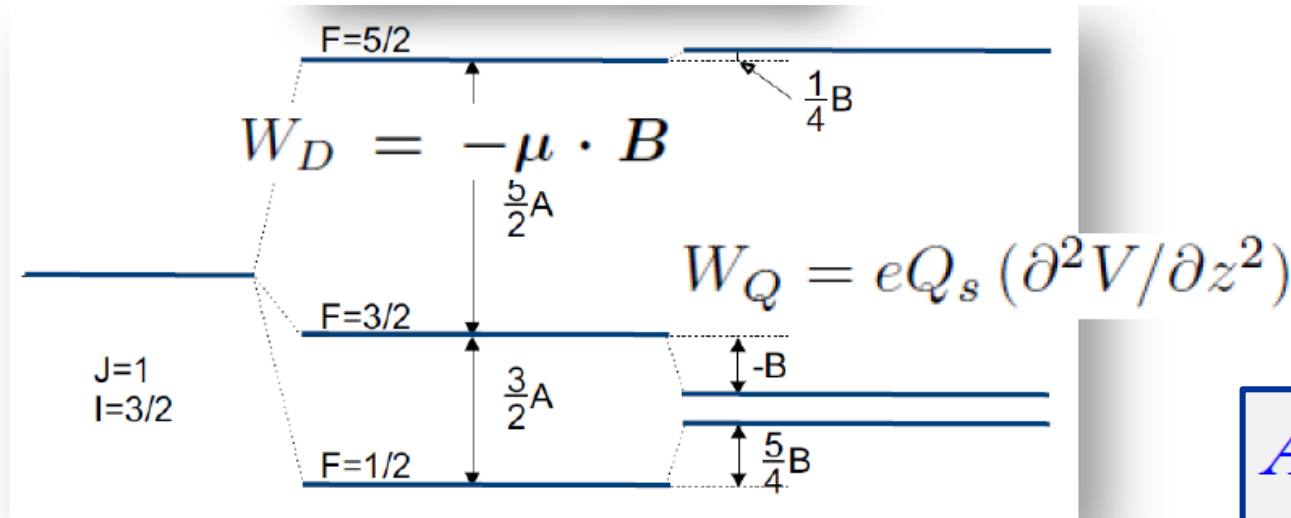
→ Mean squared nuclear charge radius difference and deformation β



From Hyperfine Structure to the Nuclear Moments μ_I and Q_s

Atomic Level Splittings by Coupling of Electron Angular Momentum J and Nuclear Spin I via the Moments μ_I and Q_s

$$\vec{F} = \vec{I} + \vec{J} \quad (|I - J| \leq F \leq I + J)$$



Nuclear Magnetic
Dipole Moment μ_I



$$A = \mu_I B_e(0) / (IJ)$$

$$B = eQ_s V_{ZZ}(0)$$



Nuclear Electric

Quadrupole Moment Q_s

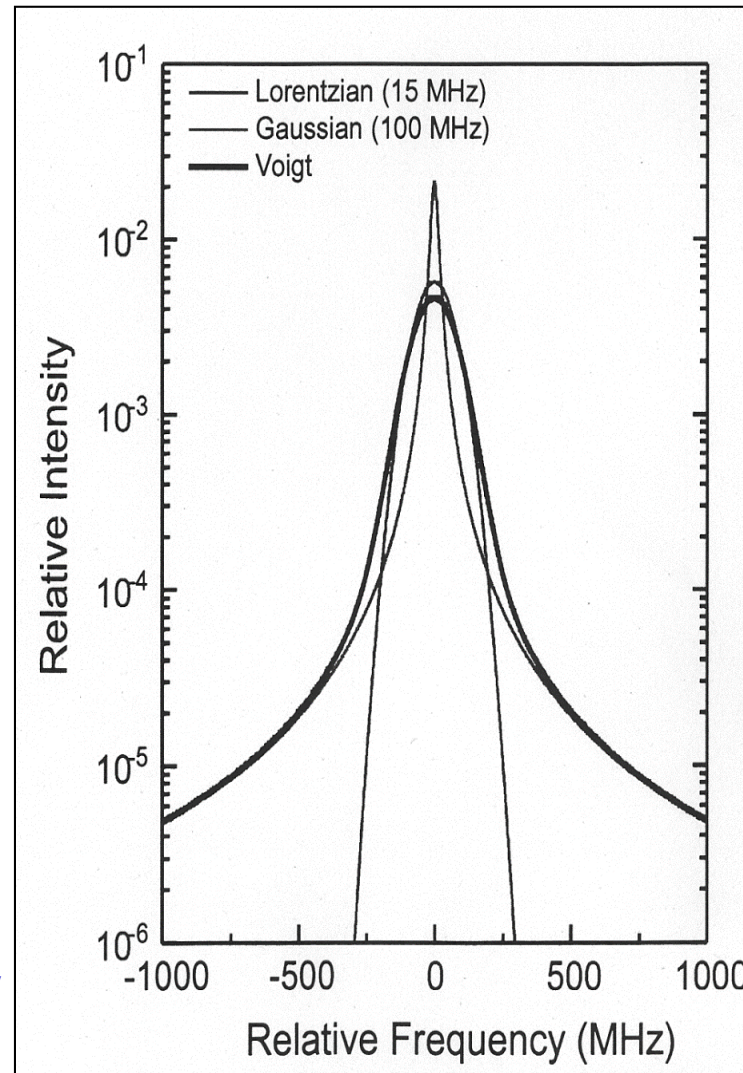
$$W_F = \frac{1}{2}AC + B \frac{\frac{3}{4}C(C+1) - I(I+1)J(J+1)}{2I(2I-1)J(2J-1)}$$

$$C = F(F+1) - I(I+1) - J(J+1).$$

Spectral Considerations for Narrowband Laser Excitation

Resolution in laser spectroscopy determined by

- Single free atom at rest → natural linewidth = **Lorentzian of ~10 MHz**
- Ensemble of thermally moving atoms in vapor → **Gaussian 500 MHz – 5 GHz**
- Additional contribution from laser line width → **Gaussian 1 MHz(cw) – 5 GHz(pulsed)**
- Strong linewidth suppression down to natural linewidth by fast beam **Doppler** compression in **collinear laser spectroscopy** (on ions, atoms or molecules)



Lorentzian (homogeneous)

$$L(\nu) = \frac{1}{\pi[w_L + (\nu_0 - \nu)^2 / w_L]}$$

$$w_L = HWHM = \frac{1}{4\pi\tau}$$

Gaussian (inhomogeneous)

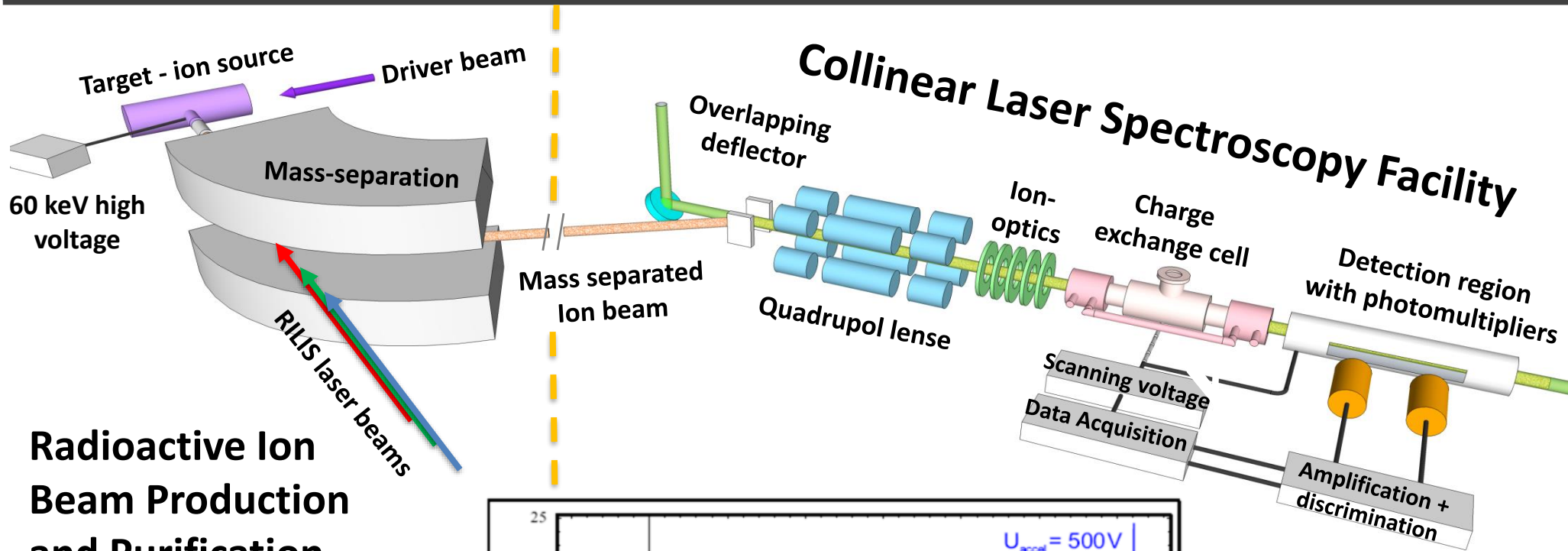
$$G(\nu) = \frac{1}{w_G \sqrt{\pi}} \exp[-(\nu_0 - \nu)^2 / w_G^2]$$

$$w_G = HW \frac{1}{e} = 4.3 \times 10^{-7} \nu_0 \sqrt{T / M}$$

Voigt (convolution)

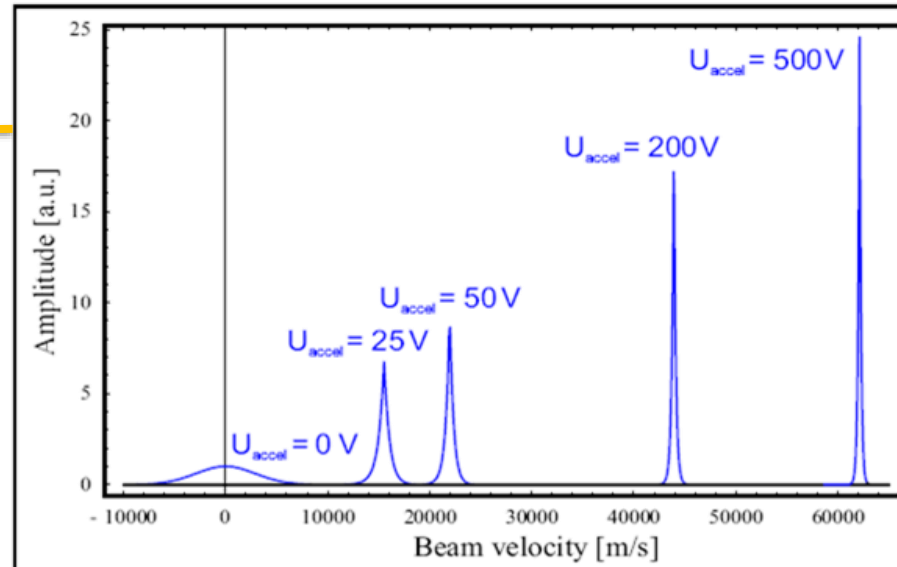
$$V(\nu) = \int_{-\infty}^{\infty} G(\nu') L(\nu - \nu') d\nu'$$

Principles of Collinear Laser Spectroscopy



Radioactive Ion Beam Production and Purification

$$v_{Ion} = v_{Laser} \cdot \gamma \cdot \left(1 - \frac{v}{c}\right)$$



$$E = eU = \frac{1}{2}mv^2$$

$$\delta E = mv \delta v$$

The Cradle of Collinear Laserspectroscopy...

at the **MAFIA** on-line separator of the TRIGA Research Reactor of UMz in 1978

AN ON-LINE MASS SEPARATOR FOR FISSION-PRODUCED ALKALI ISOTOPES

L. VON REISKY *, J. BONN, S.L. KAUFMAN **, L. KUGLER, E.-W. OTTEN, J.-M. RODRIGUEZ, K.P.C. SPATH and D. WESKOTT

Institut für Physik

Nu

© N

Collinear Laser Spectroscopy on Fast Atomic Beams

K.-R. Anton, S. L. Kaufman,^(a) W. Klempt, G. Moruzzi,^(b) R. Neugart, E.-W. Otten, and B. Schinzler

Institut für Physik, Johannes Gutenberg-Universität, D-6500 Mainz, Federal Republic of Germany

Phys. Rev. Lett. 40 (1978) 642

Z. Physik A 289, 227–228 (1979)

Short Note

Hyperfine Structure and Isotope Shifts of Neutron-Rich $^{138-142}\text{Cs}$

J. Bonn, W. Klempt, R. Neugart, E.-W. Otten, and B. Schinzler
Institut für Physik, Johannes Gutenberg Universität, Jakob-Welder-Weg
Mainz,
Federal Republic of Germany

PHYSICS LETTERS

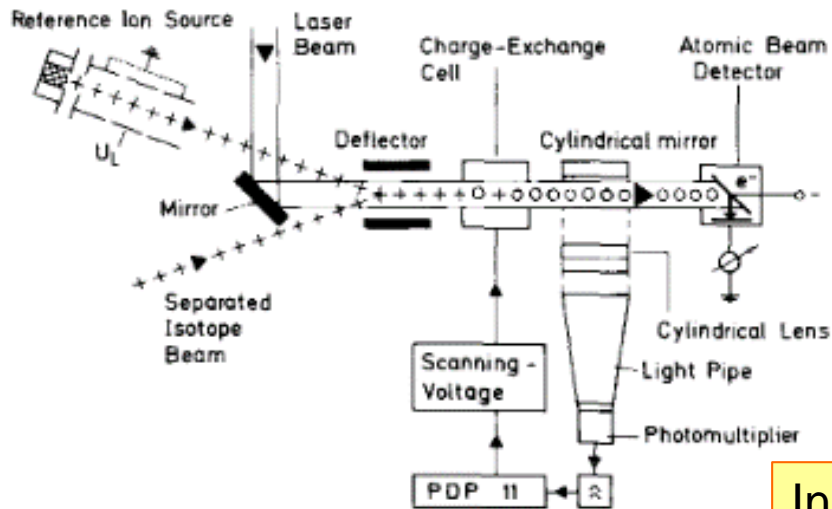
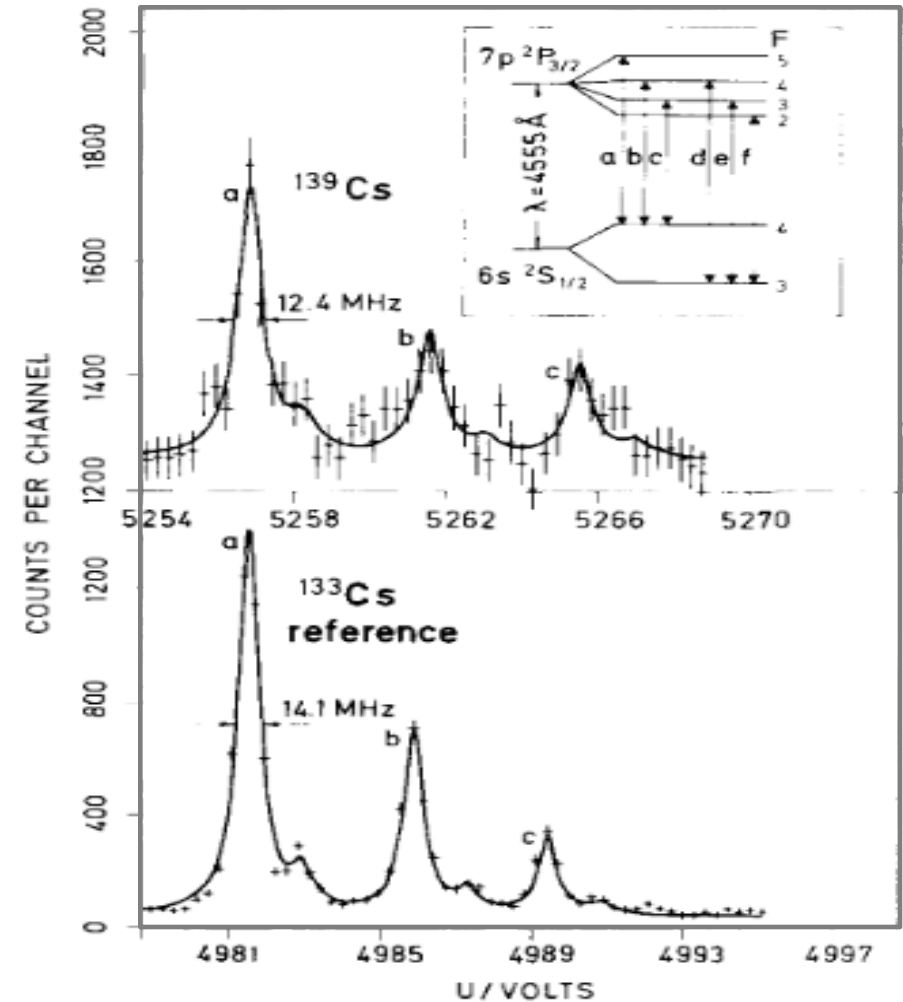
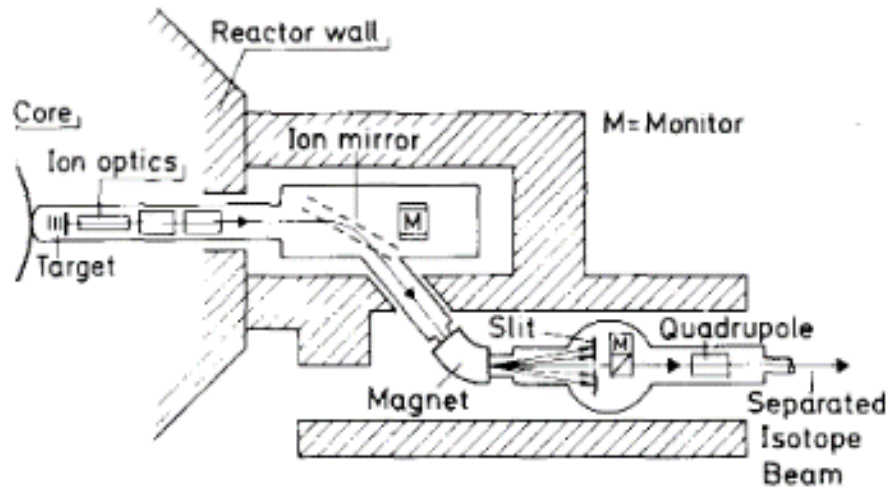
Volume 79B, number 3

COLLINEAR LASER SPECTROSCOPY OF NEUTRON-RICH Cs ISOTOPES AT AN ON-LINE MASS SEPARATOR

B. SCHINZLER, W. KLEMPT, S.L. KAUFMAN¹, H. LOCHMANN,
G. MORUZZI², R. NEUGART, E.-W. OTTEN, J. BONN,
L. VON REISKY, K.P.C. SPATH, J. STEINACHER and D. WESKOTT
Institut für Physik, Universität Mainz, Germany

20 November 1978

The first Hyperfine Structure Spectra in Radiocesium



In reactor core ion source limited to alkaline elements
 → Transfer of CLS to ISOLDE CERN in 1980

The Prosperous First 10 Years of CLS at ISOLDE/CERN

1982

0 **Fast-Beam Laser Spectroscopy on Metastable Atoms applied to Neutron-Deficient Ytterbium Isotopes**

F. Buchinger, A.C. Mueller, B. Schinzler, K. Wendt,
C. Ekström, W. Klempt, and R. Neugart,
Nuclear Instruments and Methods **202**, 159-165 (1982)

Yb

1983

1 **Spins, Moments and Charge Radii of Barium Isotopes in the Range of $^{122-146}\text{Ba}$ determined by Collinear Fast-Beam Laser Spectroscopy**

A.C. Mueller, F. Buchinger, W. Klempt and E.W. Otten, R. Neugart, C. Ekström,
J. Heinemeier and The ISOLDE Collaboration,
Nuclear Physics A403 (1983) 234-262

Ba

2 **Nuclear Moments and Charge Radii of Rare-Earth Isotopes studied by Collinear Fast-Beam Laser Spectroscopy**

R. Neugart, K. Wendt, S.A. Ahmad, W. Klempt, and C. Ekström,
Hyperfine Interactions **15/16**, 181-186 (1983)

Dy

3 **Determination of Nuclear Spins and Moments in a Series of Radium Isotopes**

S.A. Ahmad, W. Klempt, R. Neugart, E.W. Otten, K. Wendt, and C. Ekström,
Phys. Lett. **133B**, 47-52 (1983)

Ra

1984

Nuclear Structure from on-line High Res Laser Spectroscopy

Data on 38 isotopic chains from resonant interaction between laser light and atoms

One-atom-at-a-time spectroscopy towards superheavy species

Verification of a nuclear sub-shell closure at $Z = 64$

Evidence for tri-axially shaped deformed nuclei

Charge radii of Halo nuclei

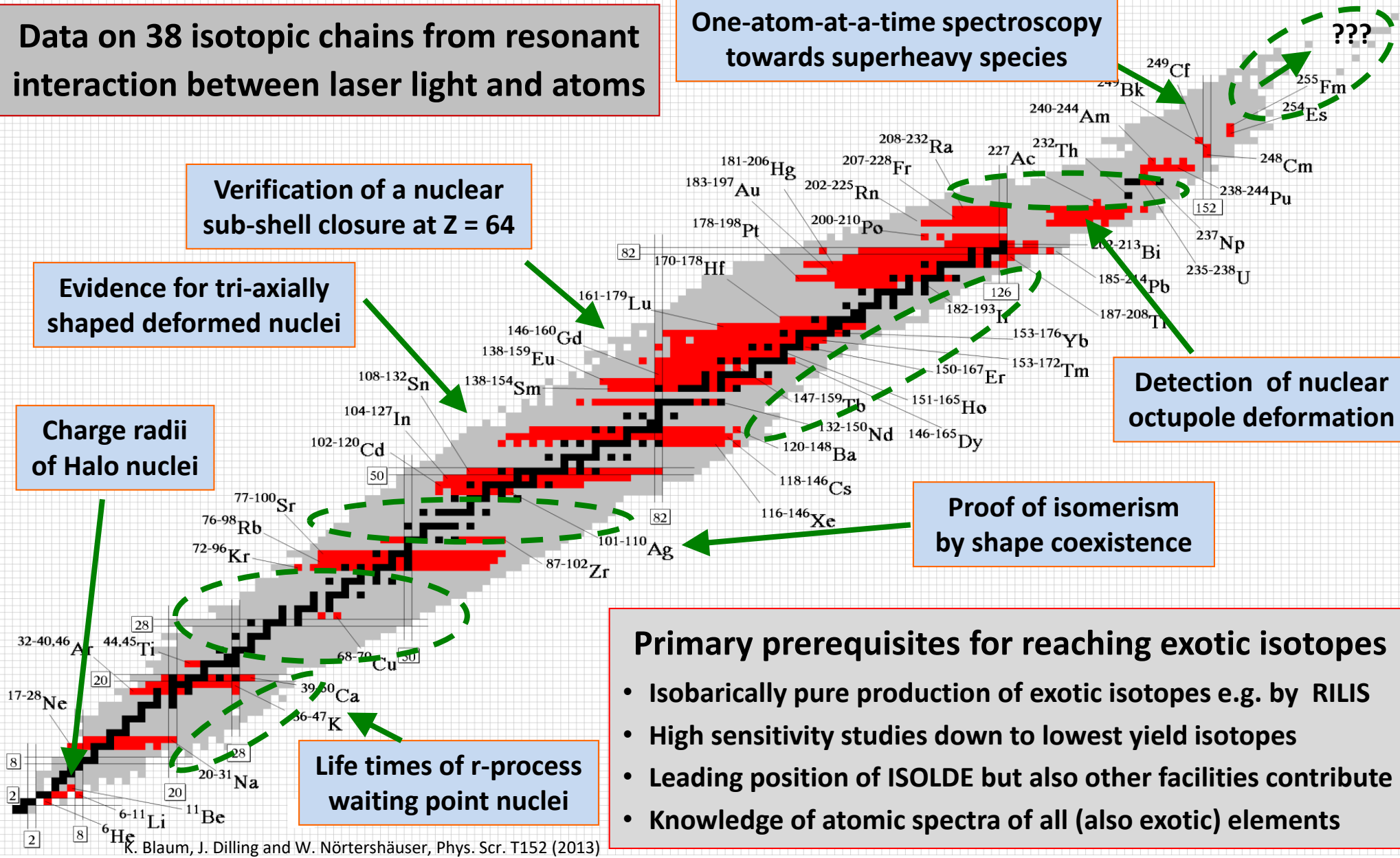
Detection of nuclear octupole deformation

Proof of isomerism by shape coexistence

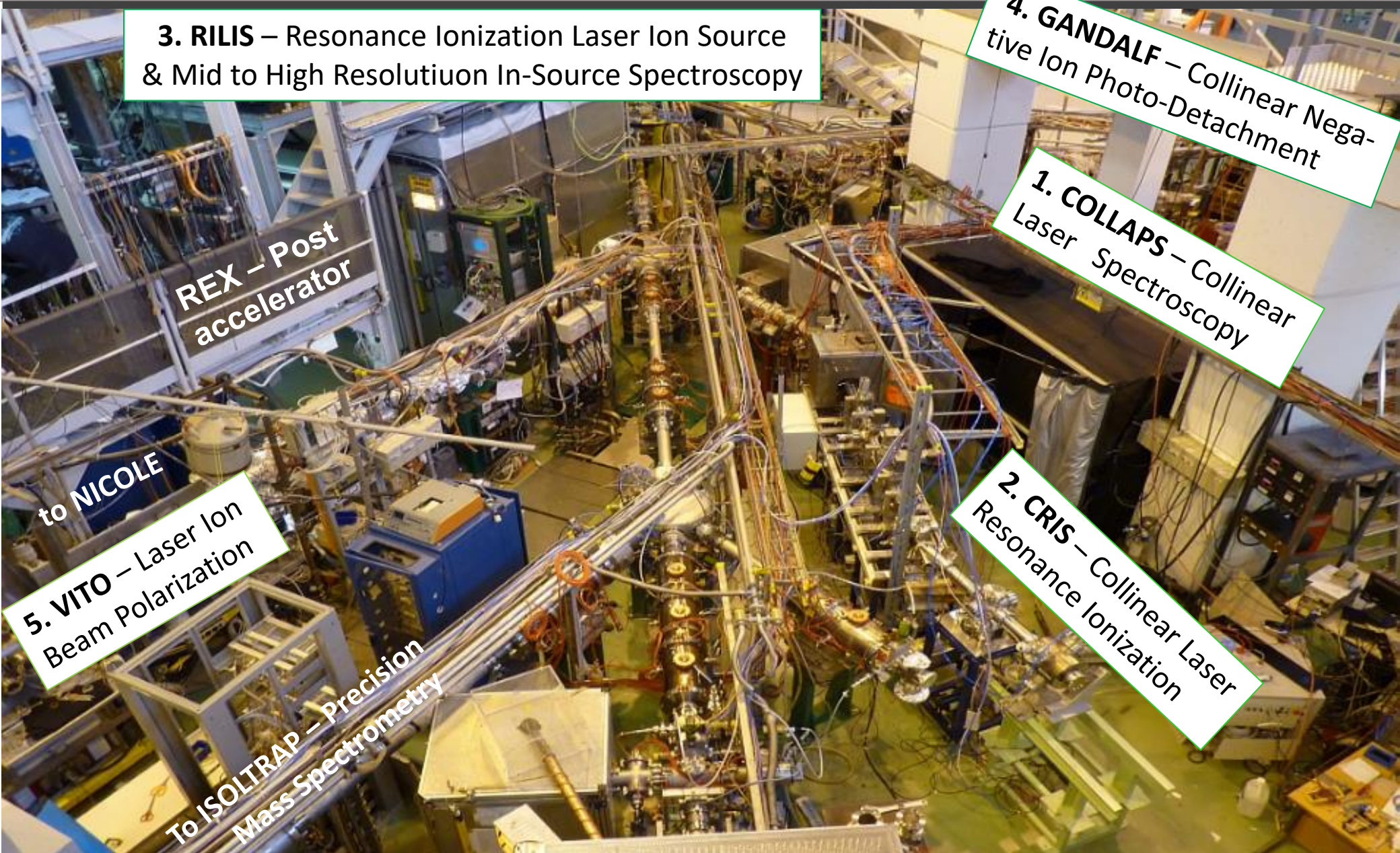
Life times of r-process waiting point nuclei

Primary prerequisites for reaching exotic isotopes

- Isobarically pure production of exotic isotopes e.g. by RILIS
- High sensitivity studies down to lowest yield isotopes
- Leading position of ISOLDE but also other facilities contribute
- Knowledge of atomic spectra of all (also exotic) elements



ISOLDE Experimental Hall with Laser & Mass Spectrometry



3. RILIS – Resonance Ionization Laser Ion Source & Mid to High Resolutiuon In-Source Spectroscopy

4. GANDALF – Collinear Negative Ion Photo-Detachment

1. COLLAPS – Collinear Laser Spectroscopy

2. CRIS – Collinear Laser Resonance Ionization

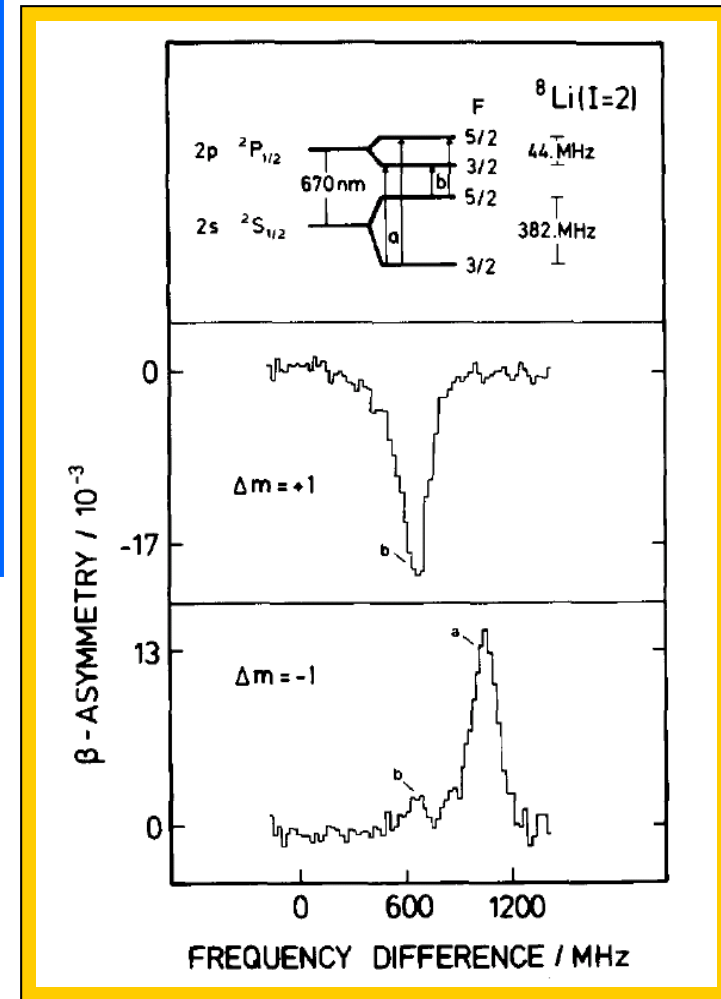
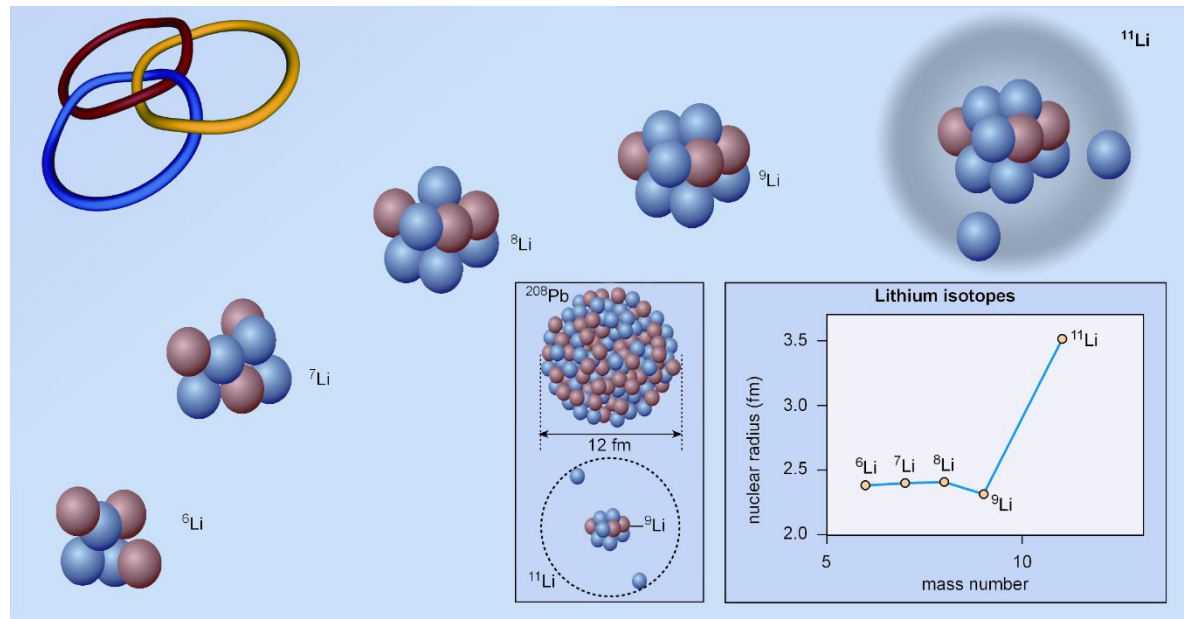
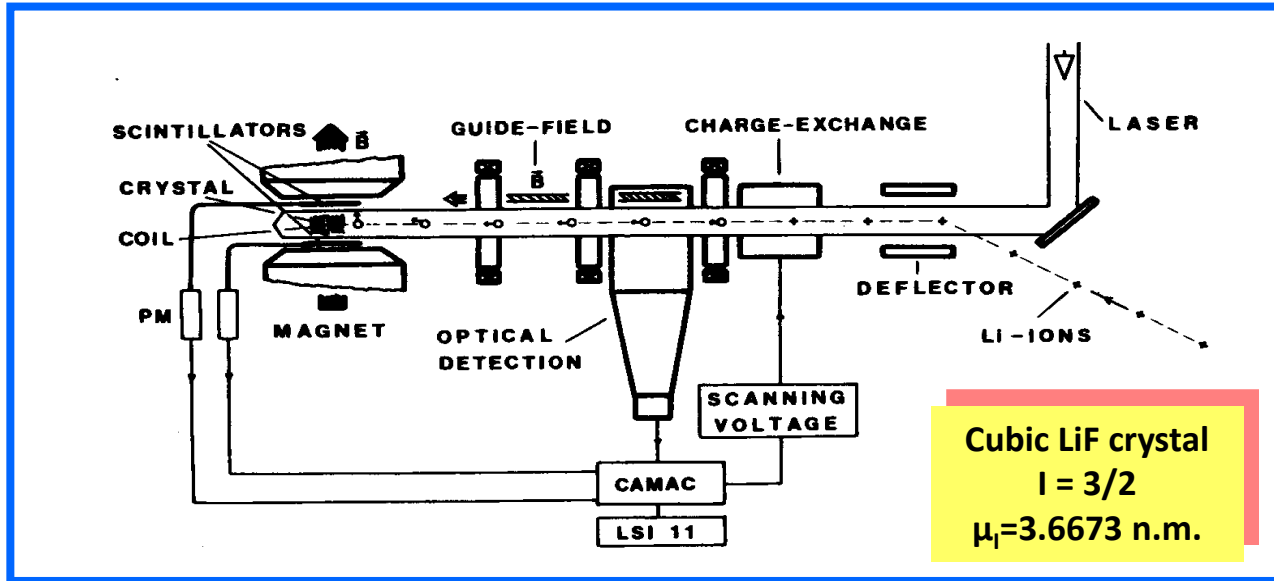
REX – Post accelerator

5. VITO – Laser Ion Beam Polarization

ISOLTRAP – Precision Mass Spectrometry

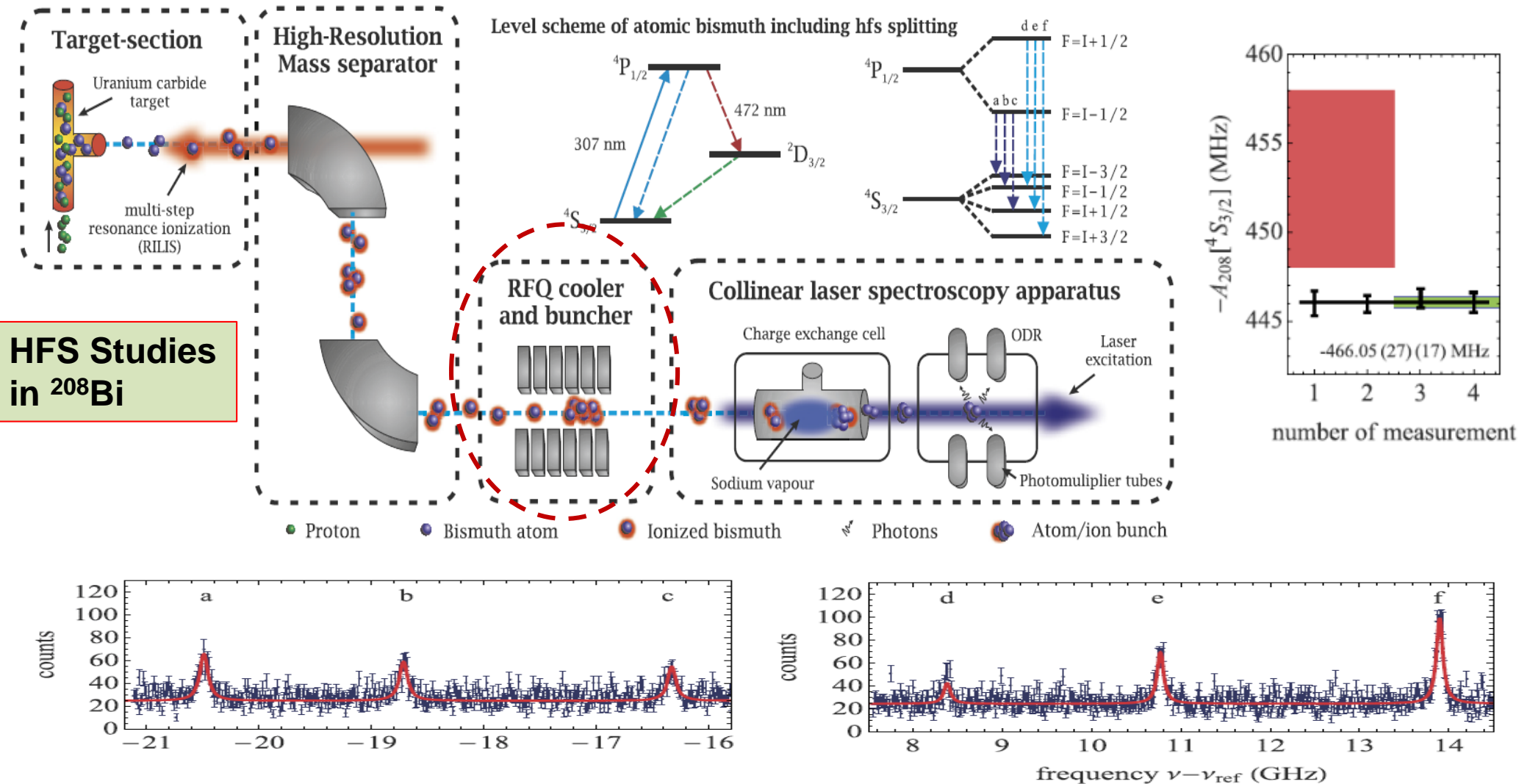
to NICOLE

Nuclear Polarization and β -NMR Detection in CLS



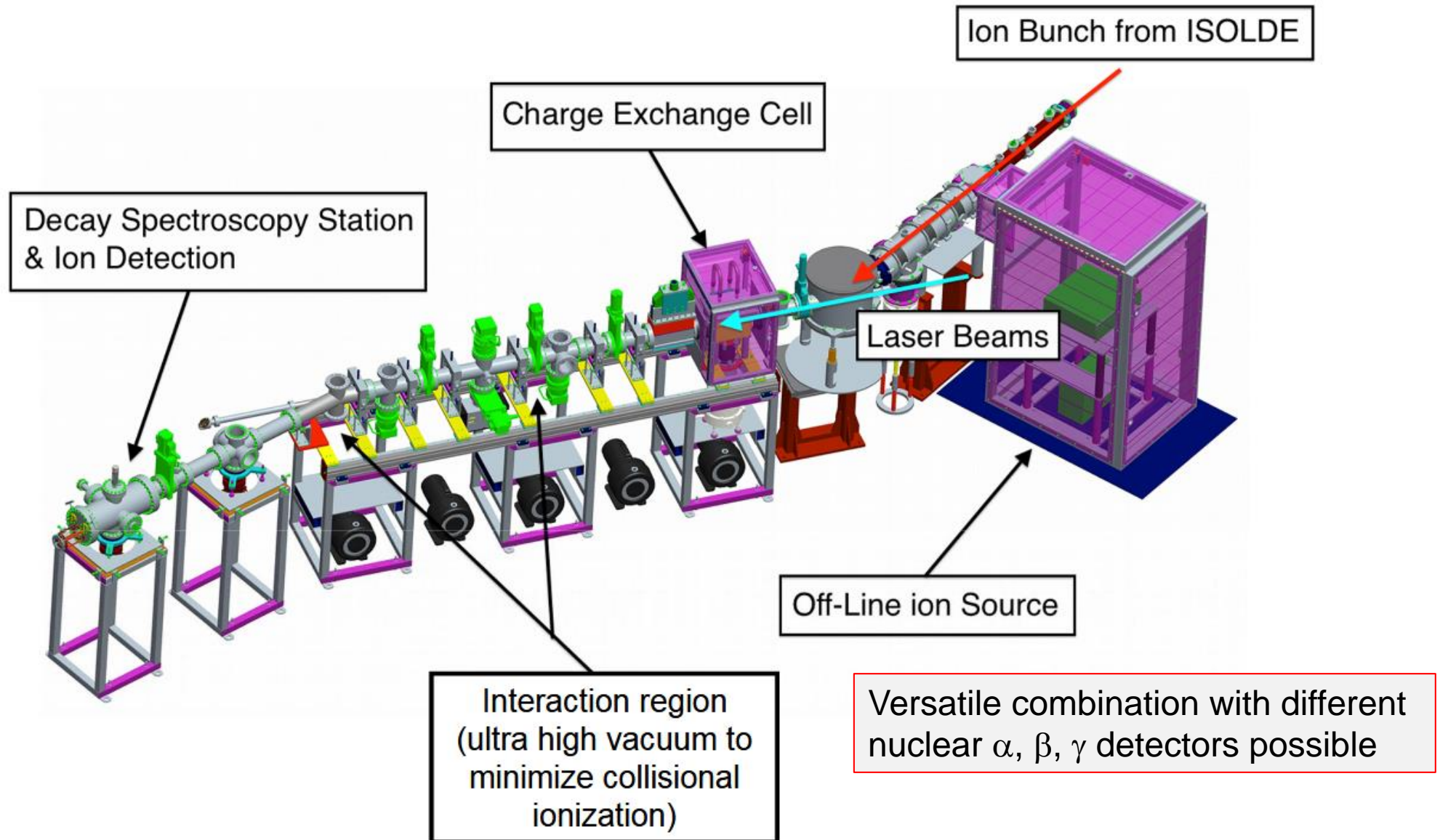
NUCLEAR SPIN AND MAGNETIC MOMENT OF ^{11}Li
 E. Arnold et al., Phys. Lett B 197, 311 (1987)

Upgrading of Collaps by Ion Beam Pulsing



The nuclear magnetic moment of ^{208}Bi and its relevance for a test of bound-state strong-field QED, S.Schmidt et al., *Physics Letters B* 779 (2018) 324–330

Resonance Ionization Detection in CLS



The CRIS Collaboration



J. Billowes, T.E. Cocolios, K.T. Flanagan, T.J. Procter, A. Smith, I. Strashnov, K.M. Lynch, S. Franchoo, V. Fedosseev, B. Marsh, G. Simpson, M. Bissell, I. Budincevic, R.P. De Groote, S. De Schepper, R.F. Garcia Ruiz, H. Heylen, J. Papuga, G. Neyens, H.H. Stroke, R.E. Rossel, S. Rothe, K. Wendt

Recent CRIS on-line Experiments

Indium:

→ Laser spectroscopy up to ^{101}In (Z=49,N=52)

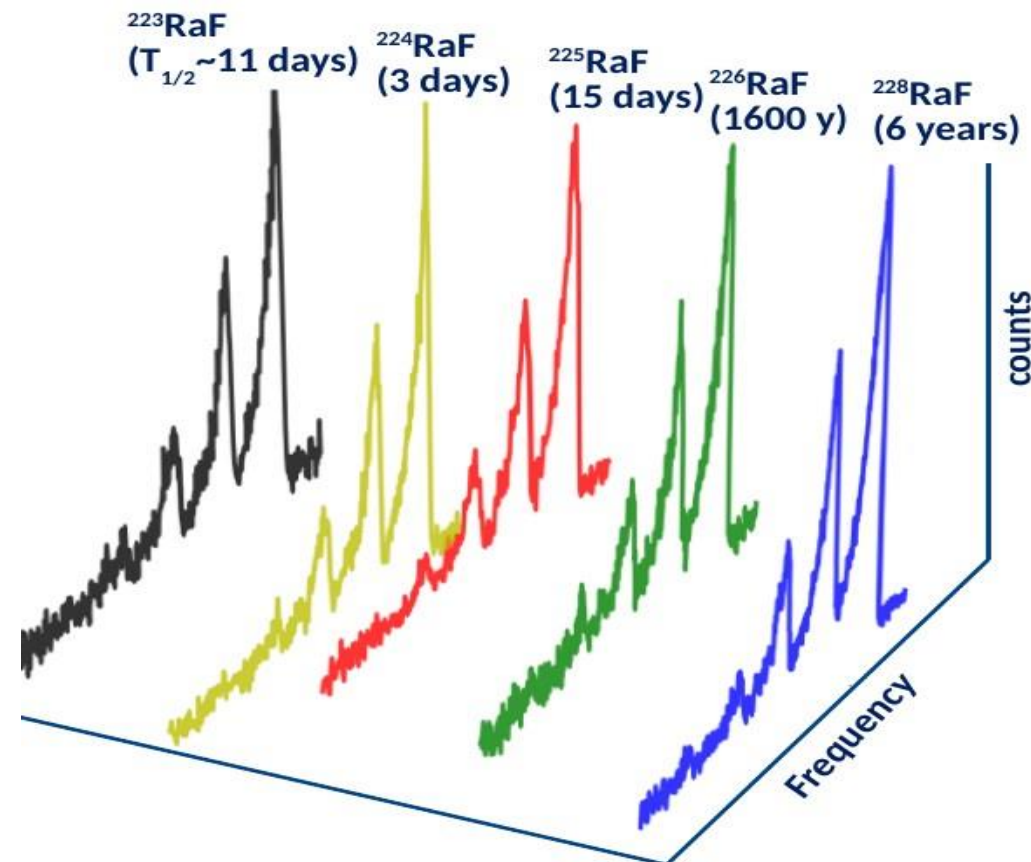
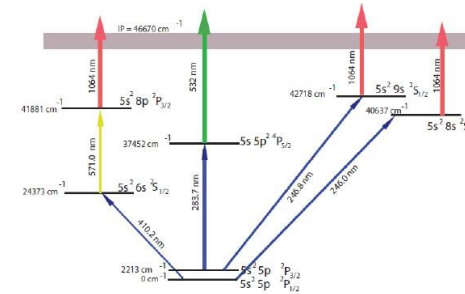
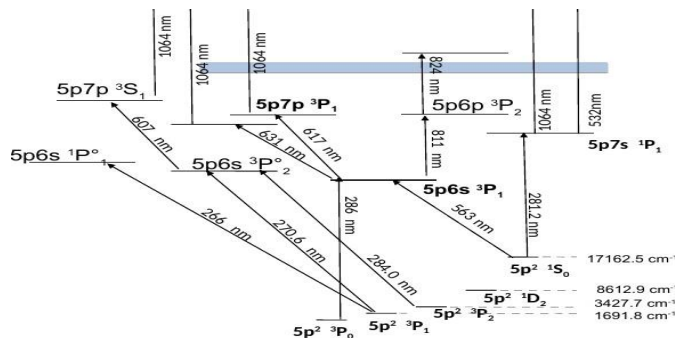
Yields ~ 100 ions/s

Potassium:

→ Laser spectroscopy of ^{52}K ($Z=19$, $N=33$)

Tin:

→ Laser spectroscopy of $^{103-122}\text{Sn}$

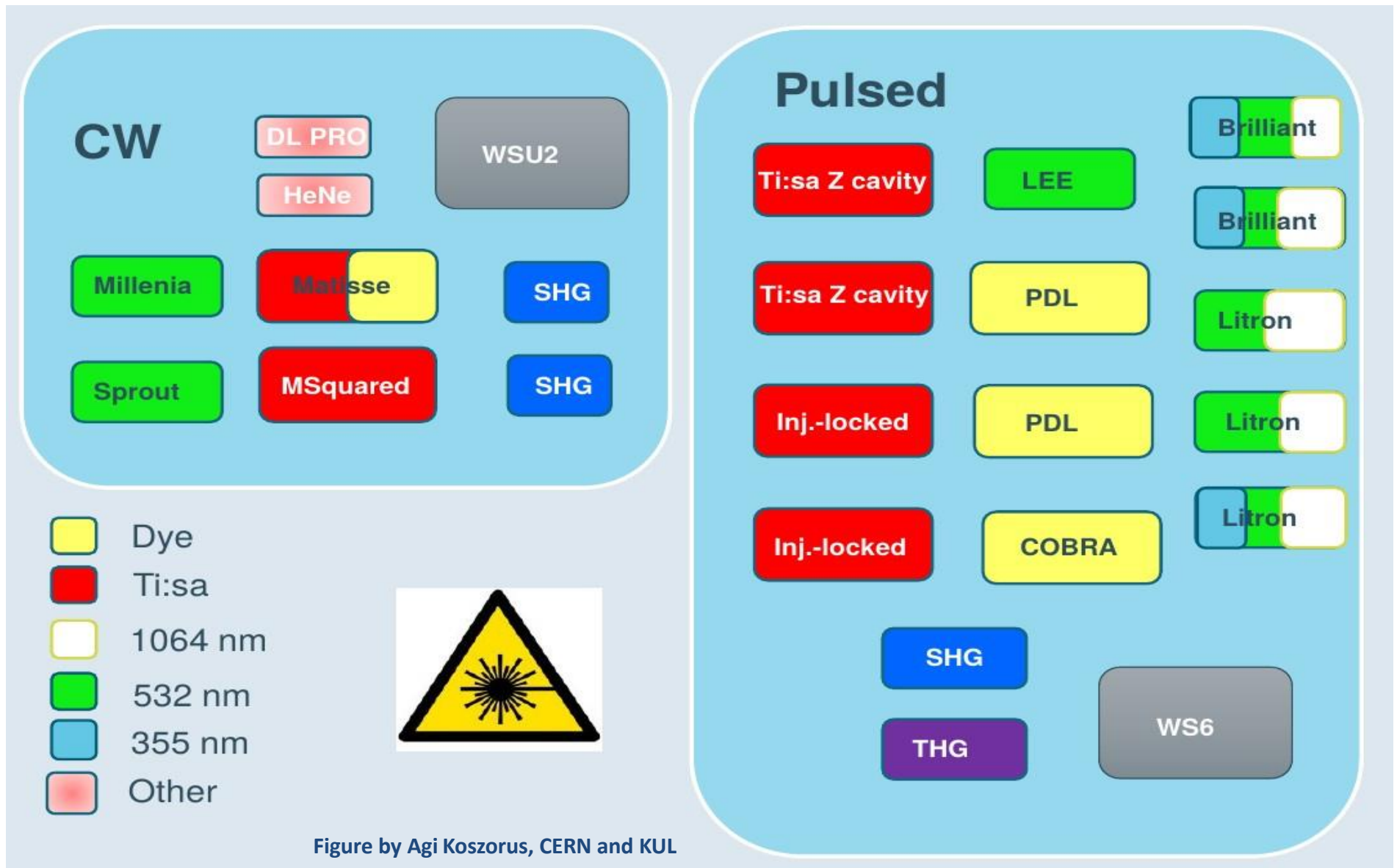


First on-line Spectroscopy on molecules

→ RaFluoride

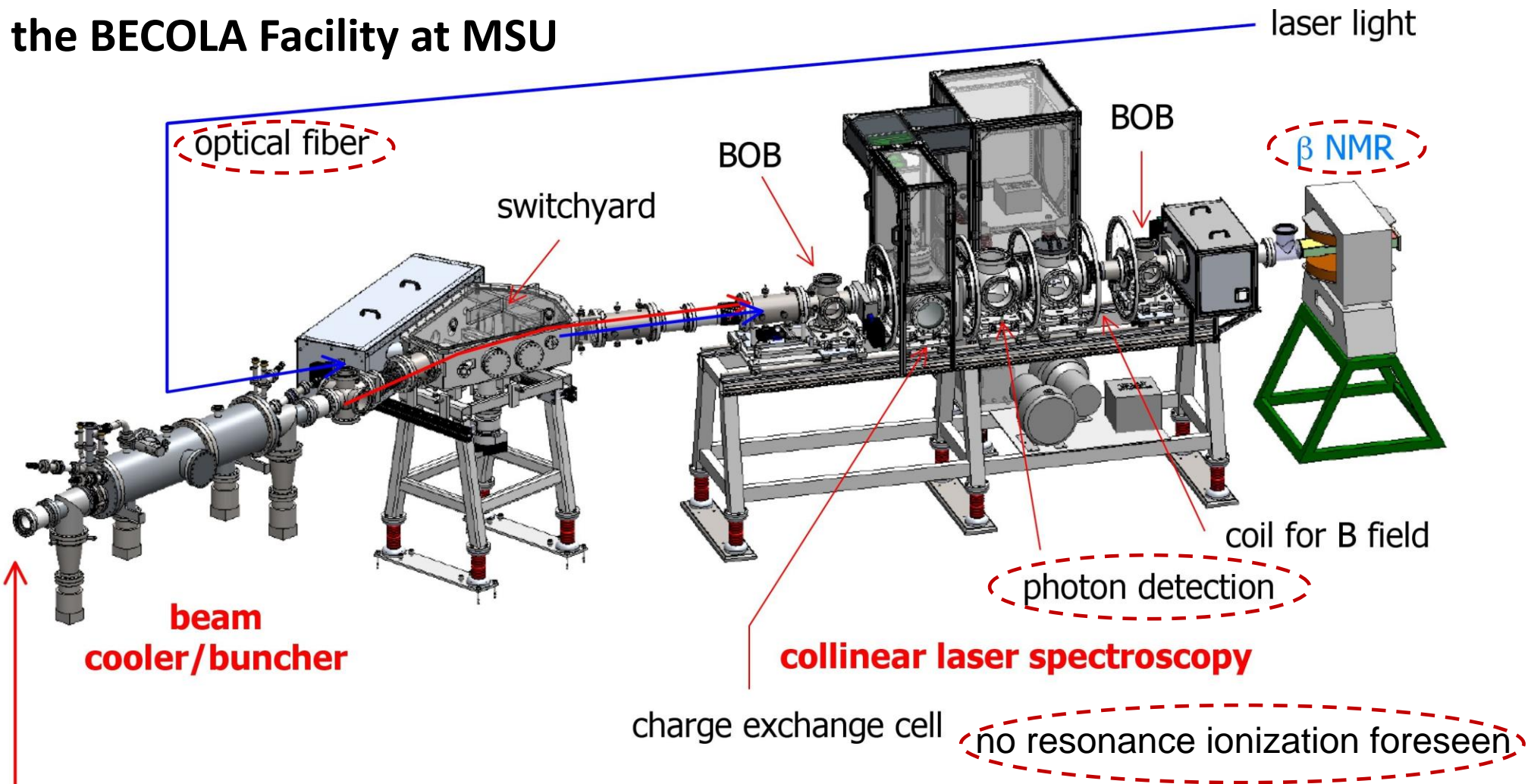
Excitation energy of low-lying levels of ^{226}RaF

The Need of a full Collection of Lasers



Collinear Laser Spectroscopy up to date

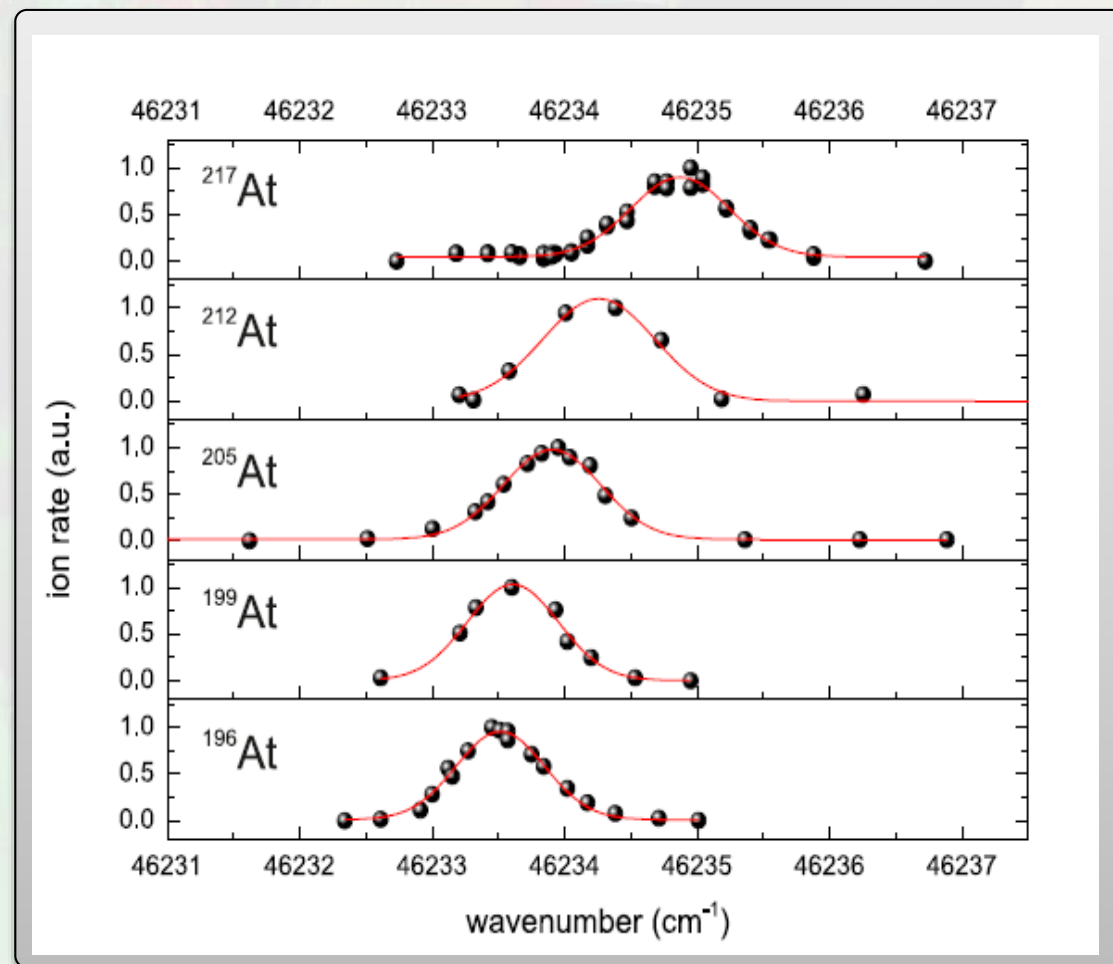
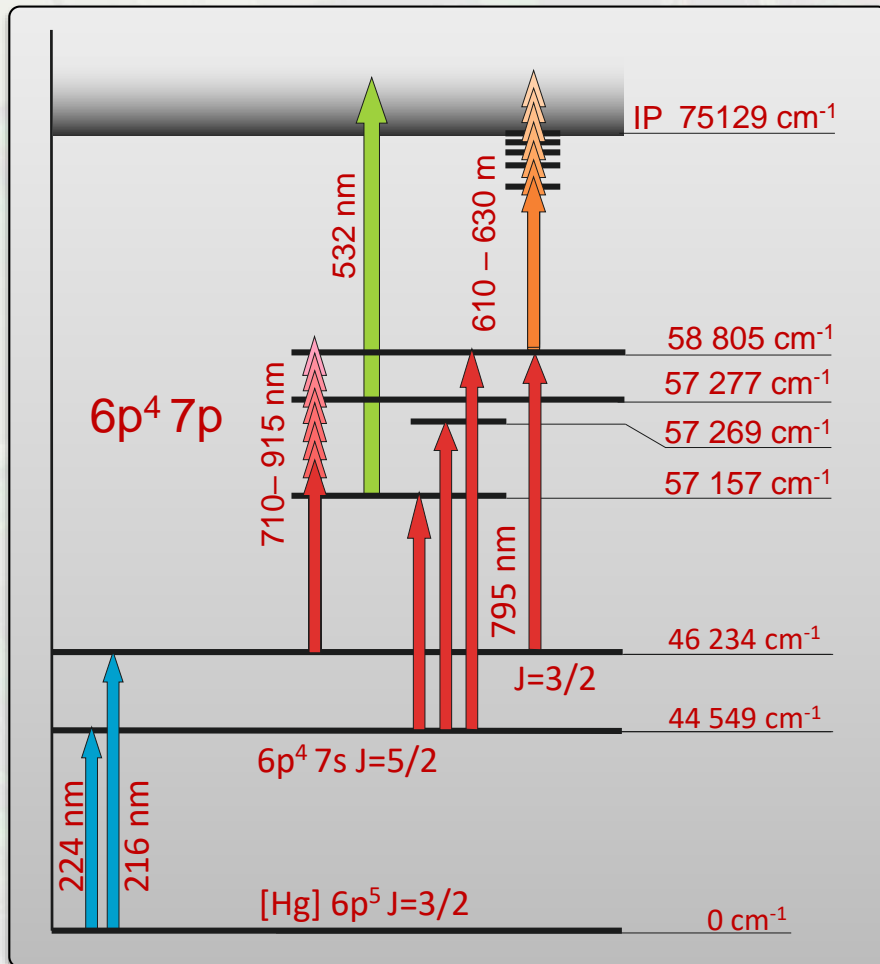
the BECOLA Facility at MSU



Commissioning of the collinear laser spectroscopy facility BECOLA at NSCL/MSU,
K. Minamisono et al., Hyp. Int. 230, 57-63 (2015)

Alternative Approaches? Mid-Resolution In-Source Spec.

- Resolution limited by **Doppler broadening** in the hot ion source and lasers (**FWHM ≈ 15 GHz**)
- **In-RILIS Spectroscopy** for **heavy elements** with large isotope shift & hyperfine structure
- Direct in-source laser spectroscopy on hyperfine structure & isotope shift of $^{196,199,205,212,217}\text{At}$

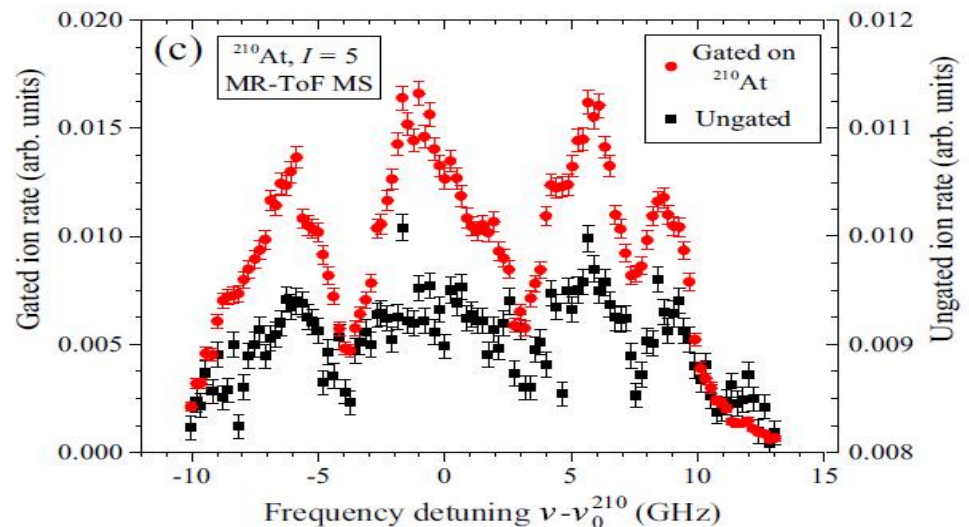
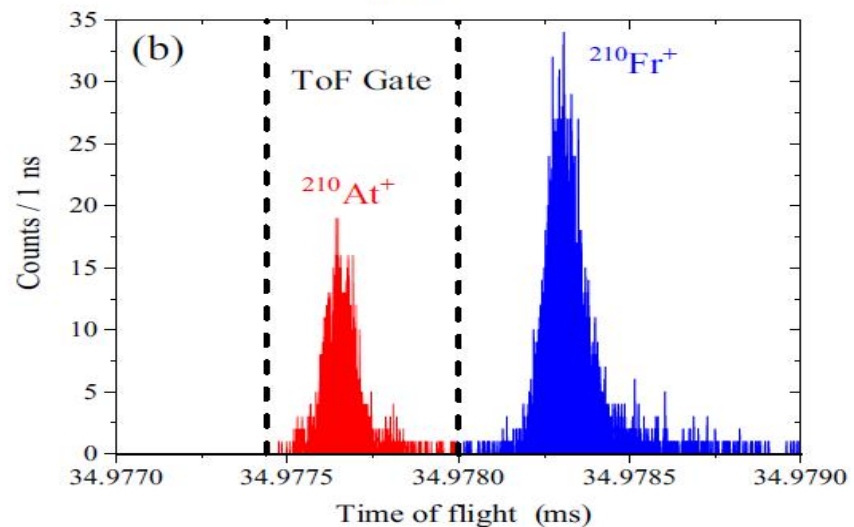
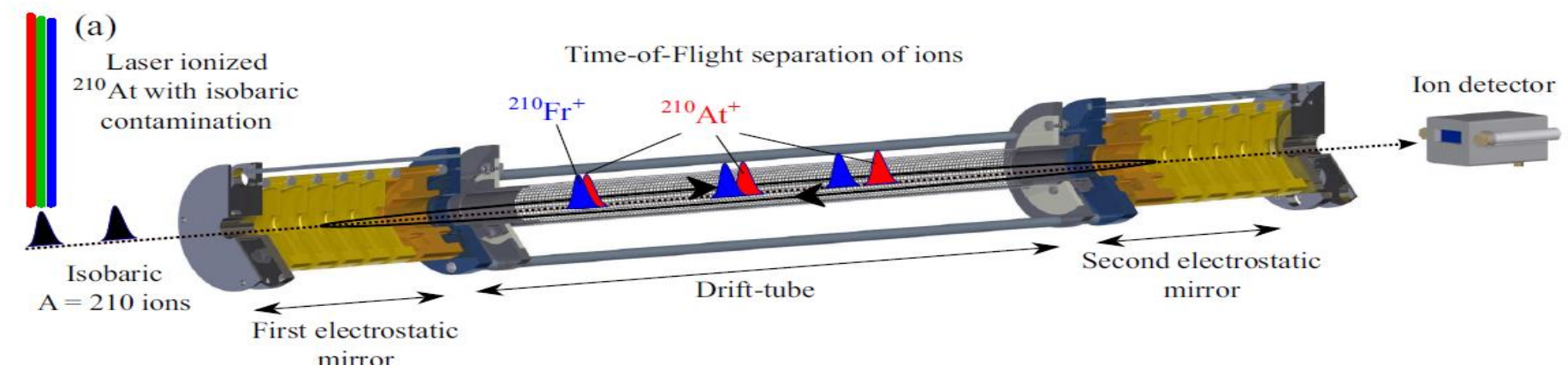


Suppression of Contaminations in In-Source Spectroscopy

	Radon			Francium		Fr 199	Fr 200	Fr 201	Fr 202	Fr 203	Fr 204	Fr 205	Fr 206	Fr 207	Fr 208	Fr 209	Fr 210	Fr 211	Fr 212	Fr 213	Fr 214	Fr 215	Fr 216	Fr 217	Fr 218	Fr 219	Fr 220	Fr 221	Fr 222	Fr 223	Fr 224	Fr 225
	86			87		16 ms	650 ms 24 ms	48 ms	340 ms 290 ms	550 ms	1.7 s 2.4 s 1.7 s	3.92 s	100 ms 160 ms 161 s	14.8 s	59.1 s	50.0 s	3.18 m	3.10 m	20.00 m	34.6 s	3.35 ms 5.0 ms	86 ns	700 ns	22 μs	22.0 ms 1.0 ms	20 ms	27.4 s	4.90 m	14.20 m	21.80 m	3.33 m	4.00 m
Astatine	At 194	At 195	At 196	At 197	At 198	At 199	At 200	At 201	At 202	At 203	At 204	At 205	At 206	At 207	At 208	At 209	At 210	At 211	At 212	At 213	At 214	At 215	At 216	At 217	At 218	At 219	At 220	At 221	At 222	At 223		
85	250 ms I=10	40 ms I=3	147 ms I=1/2	328 ms I=3/2	1.0 s I=3/2	7.2 s I=9/2	1.1 s I=1/2	1.42 m I=9/2	140 ms I=1/2	7.40 m I=9/2	108 ms I=10	26.90 m I=9/2	30.00 m I=5	1.80 h I=9/2	1.63 h I=6	5.41 h I=9/2	8.10 h I=5	7.21 h I=9/2	119 ms I=9	125 ns I=9/2	558 ns I=1	100 μs I=9/2	300 μs I=1	32.3 ms I=9/2	1.5 s I=1	54 s I=5/2	3.71 m I=3	2.30 m I=3/2	54 s	50 s I=3/2		

J. G. CUBISS *et al.*

PHYSICAL REVIEW C 97, 054327 (2018)



Nuclear Ground State Properties of At from In-RILIS Spec

Astatine	At 194	At 195	At 196	At 197	At 198	At 199	At 200
85	290 ms 147 ms 328 ms 147 ms	30 ms 183 ms 147 ms	3.7 s 1.1 s 1.1 s	1.0 s 4.3 s 1.1 s	7.2 s 1.1 s 1.1 s	1.1 s 1.1 s 1.1 s	1.1 s 1.1 s 1.1 s

J. G. CUBISS *et al.*PHYSICAL REVIEW C **97**, 054327 (2018)

TABLE II. Extracted values of the change in mean-square charge radii, the mean-square deformation extracted from the IS data (see Sec. IV C), and the magnetic and quadrupole moments for astatine isotopes. Errors due to the statistical uncertainties in the extracted hyperfine parameters in Table I are given in round brackets. Systematic uncertainties are given in curly brackets, in $\delta\langle r^2 \rangle$, stemming from the theoretical indeterminacy of the F and M factors for $\delta\langle r^2 \rangle_{A,205}$; in μ , due to the uncertainty in μ_{ref} and the HFA indeterminacy; and in Q_S , resulting from the uncertainty in the theoretical B_0/Q_S , and the experimental B_1/B_0 ratios.

Nucleus	N	I^π	$\delta\langle r^2 \rangle_{A,205} \text{ (fm}^2\text{)}$	β_{DM}	$\mu \text{ (}\mu_N\text{)}$	$Q_S \text{ (b)}$
$^{195}\text{At}^g$	110	$(1/2^+)$	$-0.171(7)\{9\}$	$0.21(2)$	$1.611(25)\{39\}$	
$^{195}\text{At}^m$	110	$(7/2^-)$	$-0.101(7)\{5\}$	$0.22(2)$	$3.714(97)\{90\}$	$-2.04(25)\{100\}$
^{196}At	111	(3^+)	$-0.262(10)\{13\}$	$0.17(2)$	$3.739(110)\{90\}$	$-0.64(13)\{35\}$
$^{197}\text{At}^g$	112	$(9/2^-)$	$-0.296(7)\{15\}$	$0.15(3)$	$3.849(45)\{54\}$	$-1.15(8)\{60\}$
$^{197}\text{At}^m$	112	$(1/2^+)$	$-0.133(7)\{7\}$	$0.19(2)$	$1.546(13)\{37\}$	
$^{198}\text{At}^g$	113	(3^+)	$-0.338(7)\{17\}$	$0.11(4)$	$4.037(94)\{97\}$	$-0.59(15)\{30\}$
$^{198}\text{At}^m$	113	(10^+)	$-0.315(7)\{16\}$	$0.12(3)$	$2.554(81)\{62\}$	$0.44(25)\{25\}$
$^{199}\text{At}^g$	114	$(9/2^-)$	$-0.265(7)\{13\}$	$0.12(3)$	$3.955(45)\{56\}$	$-0.95(8)\{50\}$
$^{199}\text{At}^m$	114	$(1/2^+)$	$-0.075(10)\{4\}$	$0.17(2)$	$1.595(38)\{39\}$	
$^{200}\text{At}^g$	115	(3^+)	$-0.293(7)\{15\}$	$0.08(4)$	$4.279(96)\{110\}$	$-0.50(8)\{50\}$
$^{200}\text{At}^{m1}$	115	(7^+)	$-0.277(7)\{14\}$	$0.09(5)$	$4.74(13)\{12\}$	$-0.96(12)\{50\}$
$^{200}\text{At}^{m2}$	115	(10^-)	$-0.258(9)\{13\}$	$0.10(4)$	$2.694(82)\{65\}$	$0.54(25)\{30\}$
^{201}At	116	$(9/2^-)$	$-0.197(7)\{10\}$	$0.10(4)$	$4.025(45)\{57\}$	$-0.96(15)\{50\}$
$^{202}\text{At}^g$	117	(3^+)	$-0.229(10)\{11\}$	$0.04(9)$	$4.16(12)\{10\}$	$-0.54(13)\{30\}$
$^{202}\text{At}^m$	117	(7^+)	$-0.201(10)\{10\}$	$0.06(6)$	$4.54(16)\{11\}$	$-0.65(13)\{30\}$
^{203}At	118	$9/2^-$	$-0.115(7)\{6\}$	$0.08(5)$	$4.021(45)\{57\}$	$-0.73(8)\{35\}$
^{204}At	119	7^+	$-0.109(7)\{5\}$	$0.05(8)$	$4.84(13)\{12\}$	$-0.62(8)\{30\}$
^{205}At	120	$9/2^-$	0	$0.08(4)$	$4.111(34)\{58\}$	$-0.61(8)\{30\}$
^{206}At	121	$(6^+)^a$	$0.020(7)\{1\}$	$0.06(6)$	$4.39(13)\{11\}$	$-0.42(10)\{20\}$
^{207}At	122	$9/2^-$	$0.115(7)\{6\}$	$0.08(4)$	$4.150(45)\{59\}$	$-0.45(8)\{25\}$
^{208}At	123	6^+	$0.155(7)\{8\}$	$0.07(4)$	$4.48(14)\{11\}$	$-0.40(25)\{20\}$
^{209}At	124	$9/2^-$	$0.240(7)\{12\}$	$0.09(3)$	$4.141(45)\{59\}$	$-0.40(8)\{20\}$
^{210}At	125	$(5)^+$	$0.295(7)\{15\}$	$0.09(3)$	$4.74(12)\{11\}$	$-0.42(12)\{20\}$
^{211}At	126	$9/2^-$	$0.372(9)\{19\}$	$0.09(2)$	$4.139(37)^b$	$-0.33(12)\{20\}$

^aFor $I = 5$, $\delta\langle r^2 \rangle_{A,205} = 0.009(7)\{1\} \text{ fm}^2$, $\mu = 4.34(12)\{11\} \mu_N$, $Q_S = -0.29(10)\{15\}$. Spin assignment for ^{206}At is discussed in Sec. V A 3.

^bReference value.

^aFor $I = 5$, $\delta\nu_{795}^{205} = -117(75) \text{ MHz}$, $A = -547(10) \text{ MHz}$, and $B = -176(66) \text{ MHz}$. Spin assignment for ^{206}At is discussed in Sec. V A 3.

Frequency detuning $\nu - \nu_0^{211}$ (GHz)

CHARGE RADII AND ELECTROMAGNETIC

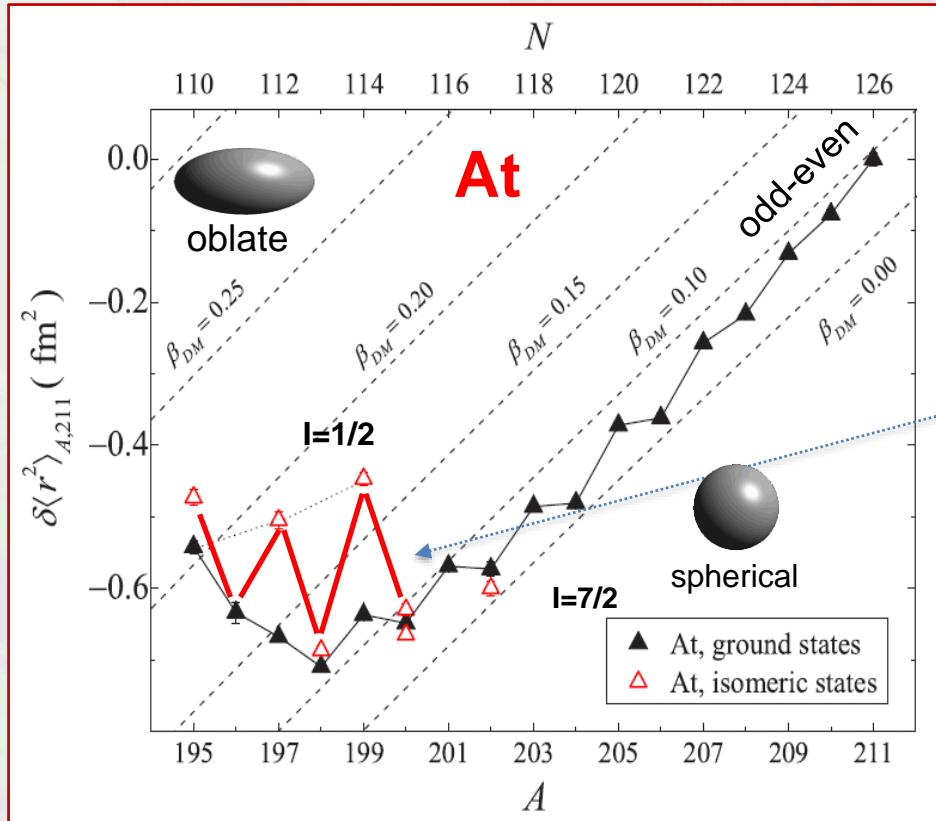
TABLE I. Measured values of the hyperfine splitting of the fitting of the hfs data are given in round brackets. The values of A -constants ratio is added. The values of

Nucleus	I^π	$T_{1/2}$
$^{195}\text{At}^g$	$(1/2^+)$	290(20) ms
$^{195}\text{At}^m$	$(7/2^-)$	143(3) ms
^{196}At	(3^+)	387(14) ms
$^{197}\text{At}^g$	$(9/2^-)$	381(6) ms
$^{197}\text{At}^m$	$(1/2^+)$	2.0(2) s
$^{198}\text{At}^g$	(3^+)	4.1(3) s
$^{198}\text{At}^m$	(10^-)	1.03(15) s
$^{199}\text{At}^g$	$(9/2^-)$	6.92(13) s
$^{199}\text{At}^m$	$(1/2^+)$	310(80) ms
$^{200}\text{At}^g$	(3^+)	43(1) s
$^{200}\text{At}^{m1}$	(7^+)	47(1) s
$^{200}\text{At}^{m2}$	(10^-)	3.5(1) s
^{201}At	$(9/2^-)$	83(2) s
$^{202}\text{At}^g$	(3^+)	184(1) s
$^{202}\text{At}^m$	(7^+)	182(2) s
^{203}At	$9/2^-$	7.4(2) min
^{204}At	7^+	9.22(13) min
^{205}At	$9/2^-$	26.9(8) min
^{206}At	$(6^+)^a$	30.6(8) min
^{207}At	$9/2^-$	1.80(4) h
^{208}At	6^+	1.63(3) h
^{209}At	$9/2^-$	5.41(5) h
^{210}At	$(5)^+$	8.1(4) h
^{211}At	$9/2^-$	7.214(7) h

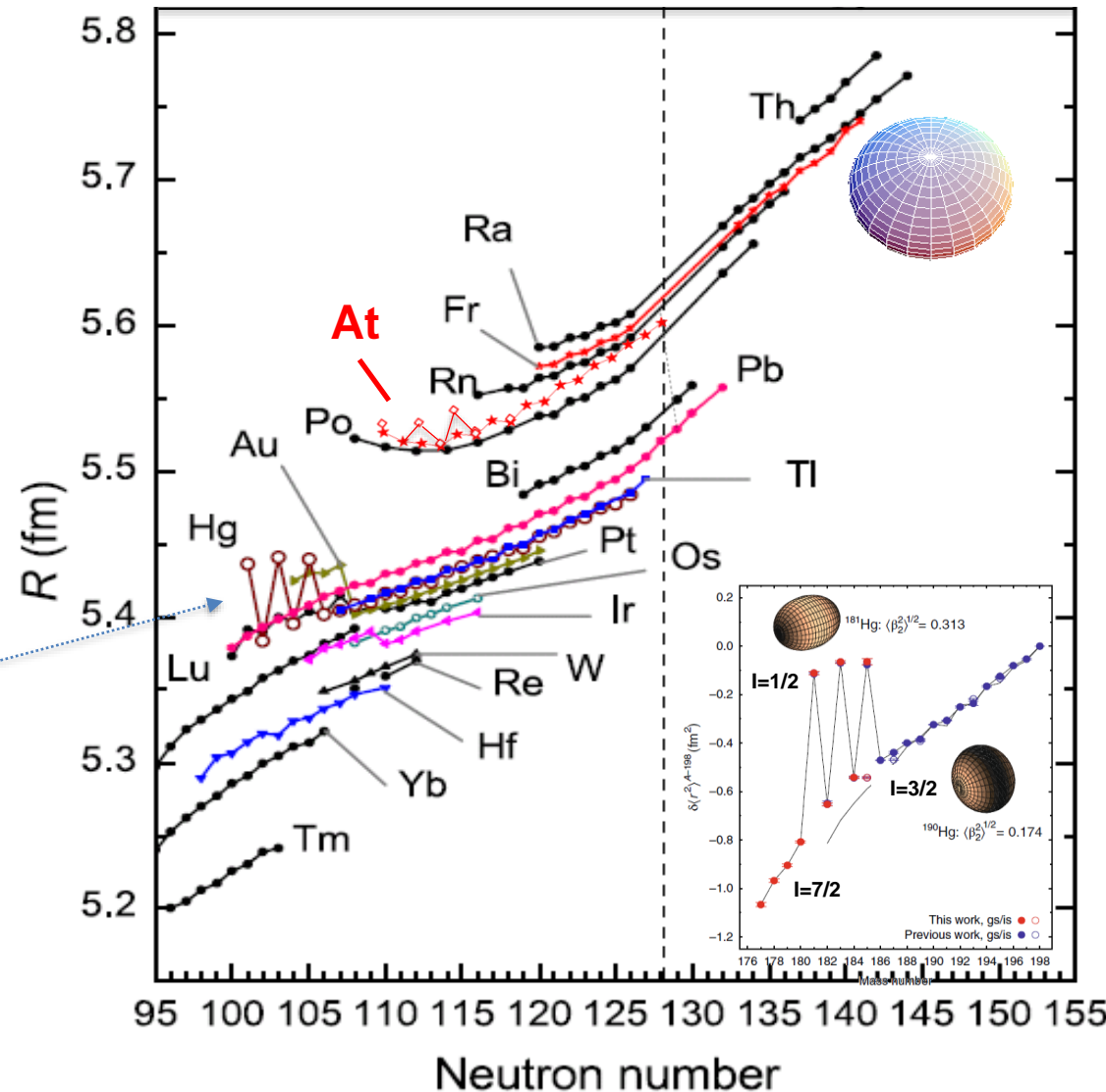
Charge Radii and Deformations in Astatine

Astatine	At 194	At 195	At 196	At 197	At 198	At 199	At 200	At 201	At 202	At 203	At 204	At 205	At 206	At 207	At 208	At 209	At 210	At 211	At 212	At 213	At 214	At 215	At 216	At 217	At 218	At 219	At 220	At 221	At 222	At 223				
85	290 ms 1/2 ⁺	147 ms 1/2 ⁺	30 ms 1/2 ⁺	37 s 1/2 ⁺	350 ms 1/2 ⁺	1.0 s 1/2 ⁺	4.3 s 1/2 ⁺	7.2 s 1/2 ⁺	1.1 s 1/2 ⁺	1.4 s 1/2 ⁺	1.42 m 1/2 ⁺	440 ms 1/2 ⁺	7.40 m 1/2 ⁺	108 ms 1/2 ⁺	9.20 m 1/2 ⁺	26.90 m 1/2 ⁺	30.00 m 1/2 ⁺	1.80 h 1/2 ⁺	1.63 h 1/2 ⁺	5.41 h 1/2 ⁺	8.10 h 1/2 ⁺	7.21 h 1/2 ⁺	119 ms 1/2 ⁺	125 ns 1/2 ⁺	558 ns 1/2 ⁺	100 μs 1/2 ⁺	300 μs 1/2 ⁺	32.3 ms 1/2 ⁺	1.5 s 1/2 ⁺	54 s 1/2 ⁺	3.71 m 1/2 ⁺	2.30 m 1/2 ⁺	54 s 1/2 ⁺	50 s 1/2 ⁺

- Ground state & isomer nuclear charge radii – almost a renaissance of the Hg shape staggering?
- Decrease in odd-even staggering points to onset of octupolar deformed nuclei around $N = 145$



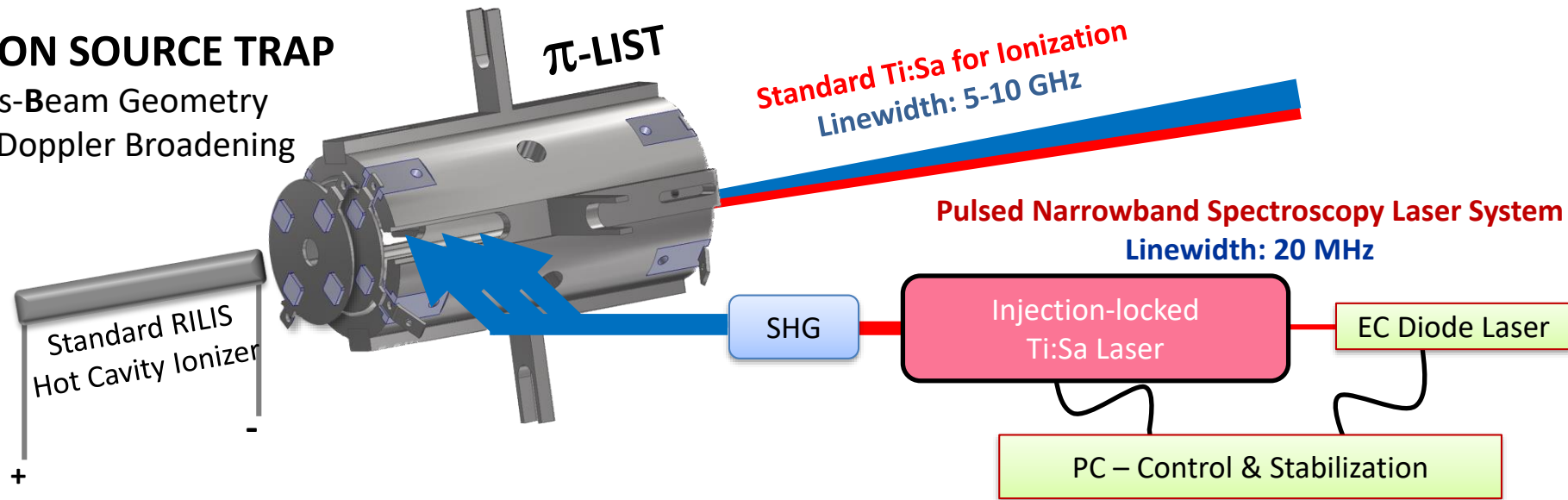
Cubiss, et al., Phys. Rev C 97, 054327 (2018)



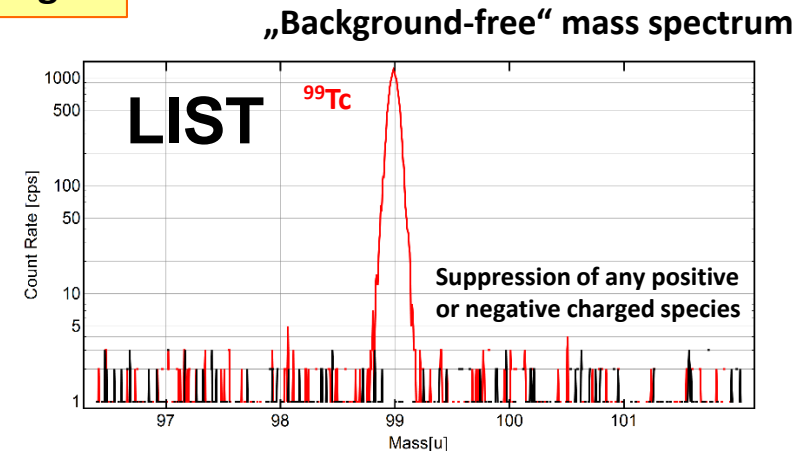
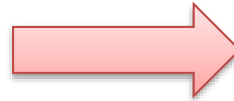
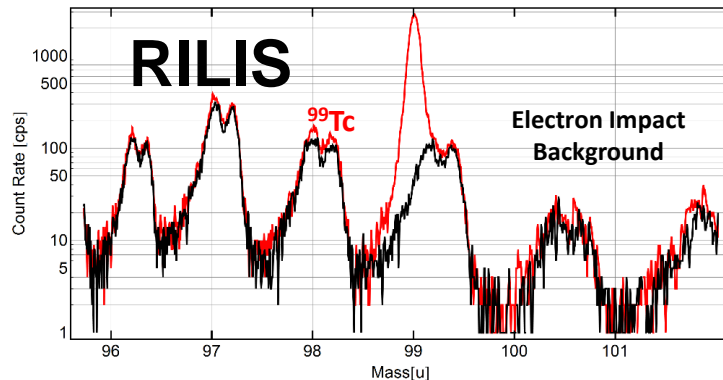
Next Generation – High-Resolution In-RILIS/LIST Spec.

LASER ION SOURCE TRAP

with Cross-Beam Geometry
prevents Doppler Broadening

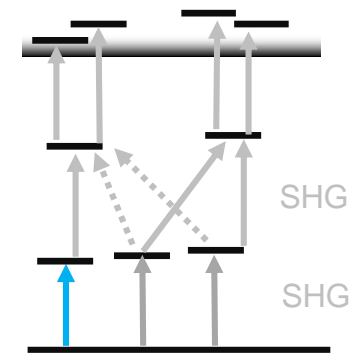
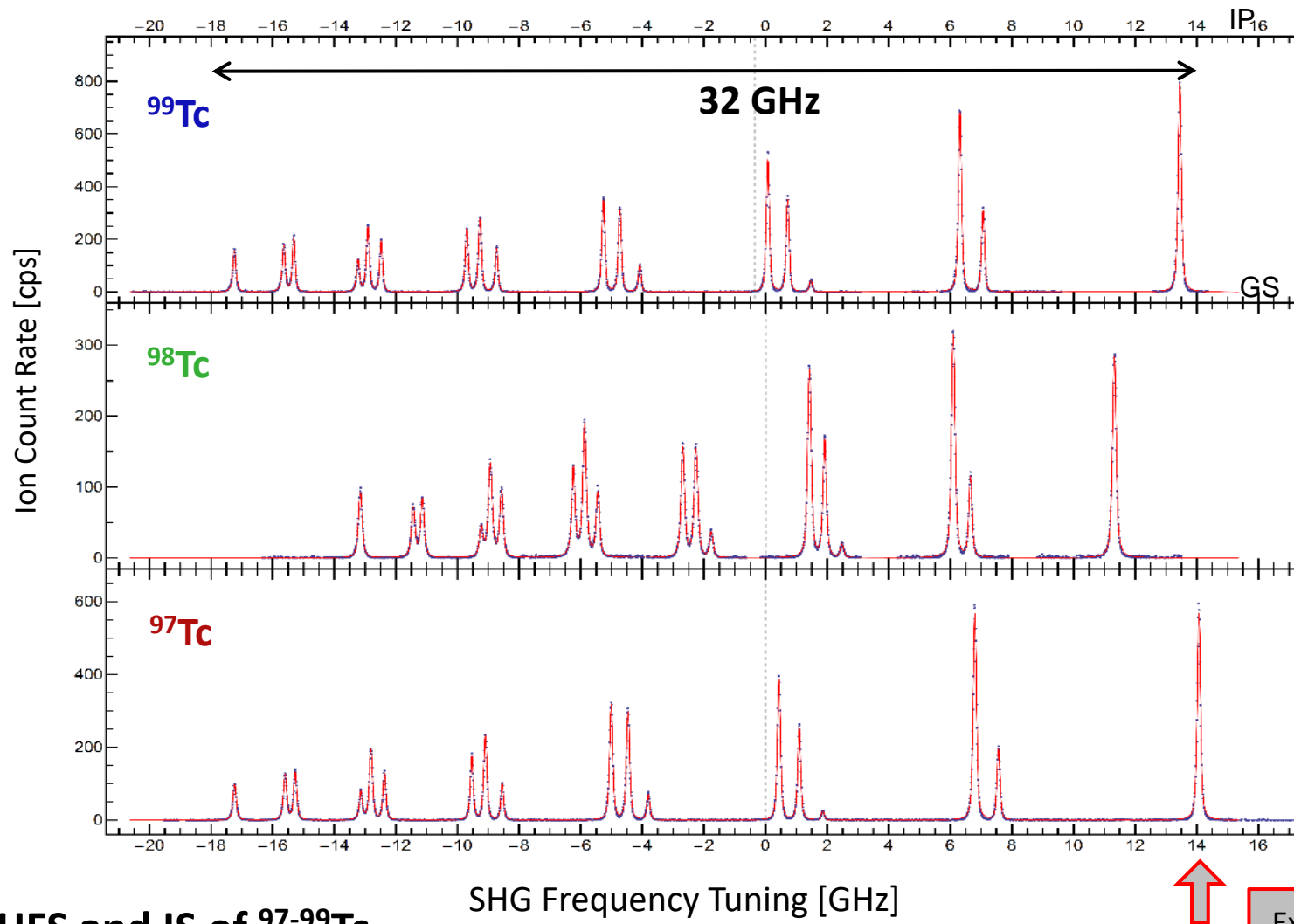


Ultimate Background Suppression by Double Repeller LIST Design



π -LIST efficiency estimated to 0.1 - 1 %

High Resolution In-LIST Spectroscopy



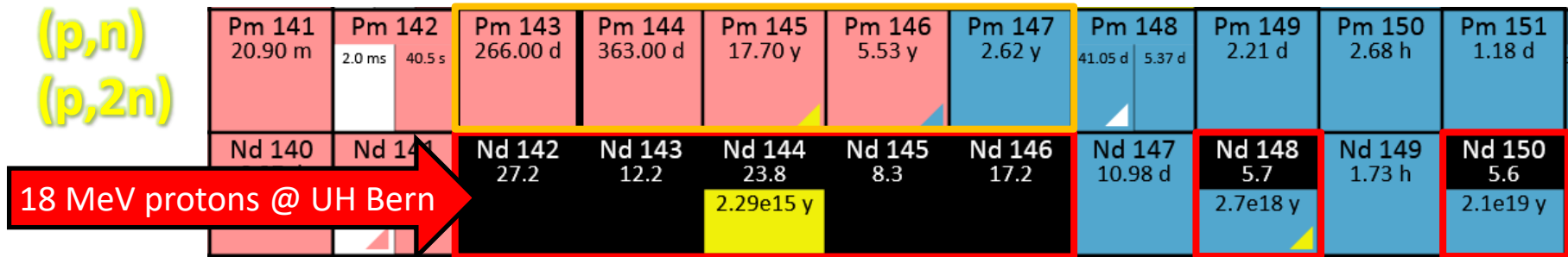
Lowest back-ground < 1 cps

Experimental linewidth ~ 50 MHz

HFS and IS of $^{97-99}\text{Tc}$

measured off-line at the RISIKO RIB facility at JGU Mz on samples $< 10^{11}$ atoms in the π -LIST

Off-line High-Resolution Laser Spec on Pm



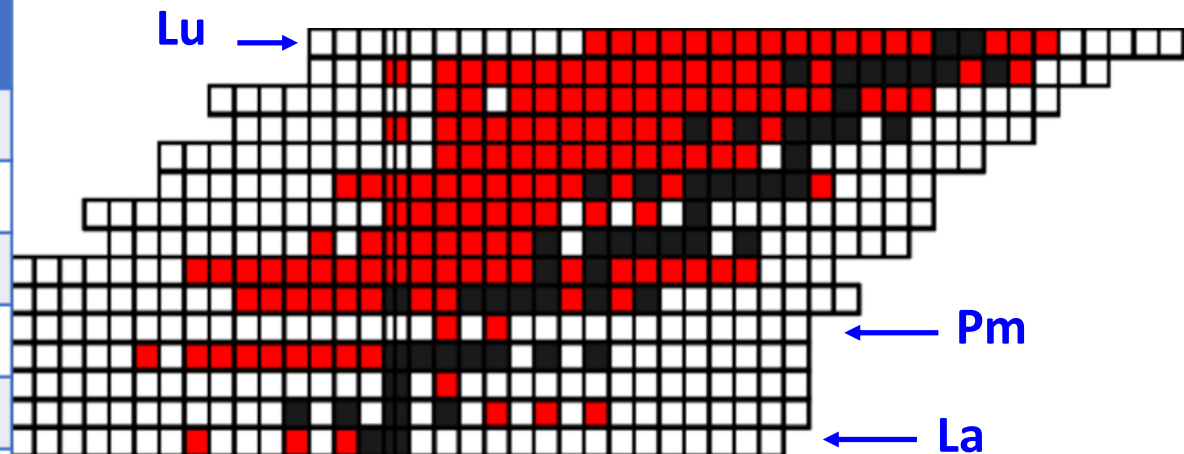
Sample specs from γ spectroscopy

Ratio Pm/Nd \approx 1/100 after radiochemistry

Isotope	Handling limit (kBq)	A total (kBq)	total atom number
Pm-143	1000	56	2.04 e12
Pm-144	1000	85	3.83 e12
Pm-145	10000	? (no γ)	?
Pm-146	1000	8.5	1.87 e12
Pm-147	10000	? (no γ)	?
Pm-148m	1000	21	1.25 e12

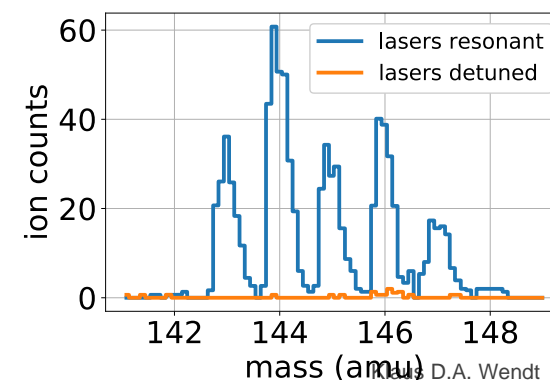
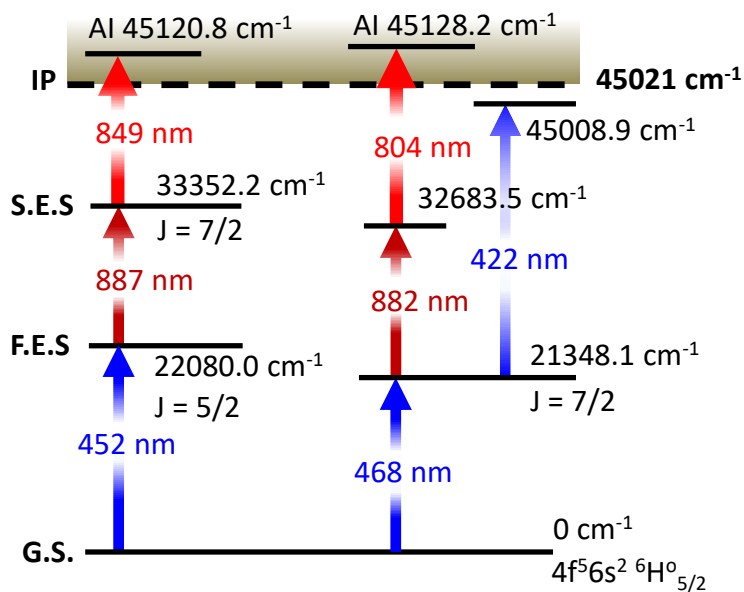
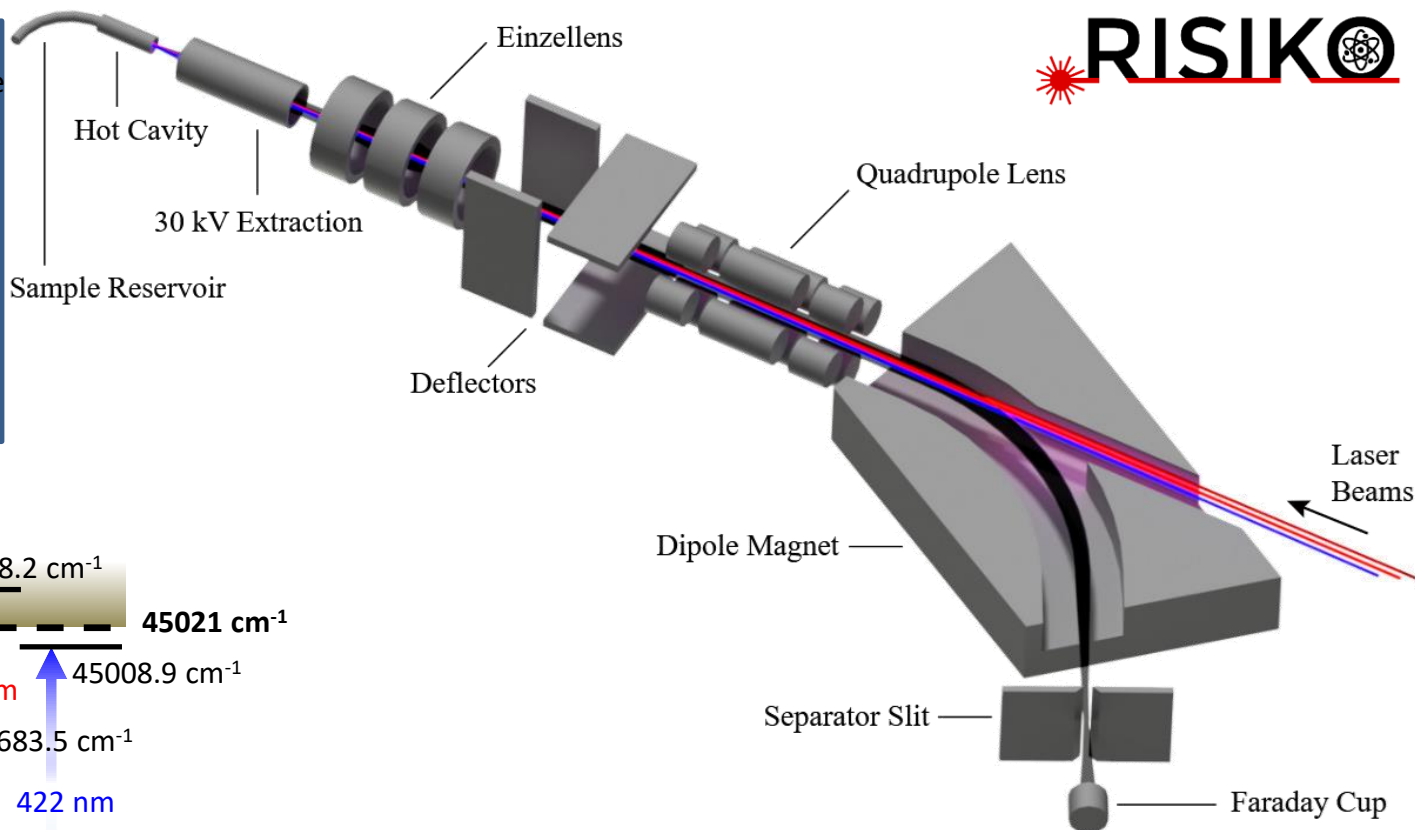
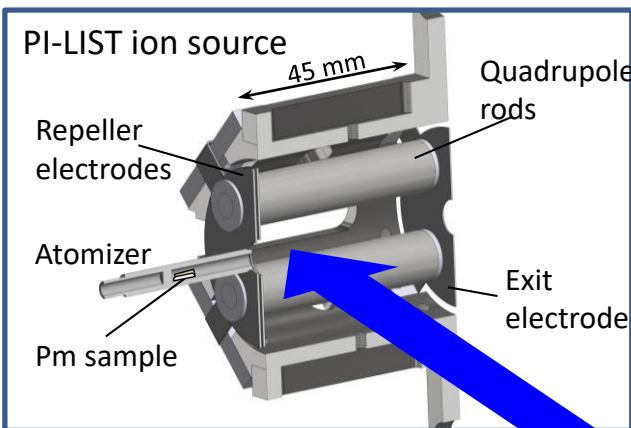
The Nuclear Chart

Cutout of the Lanthanides

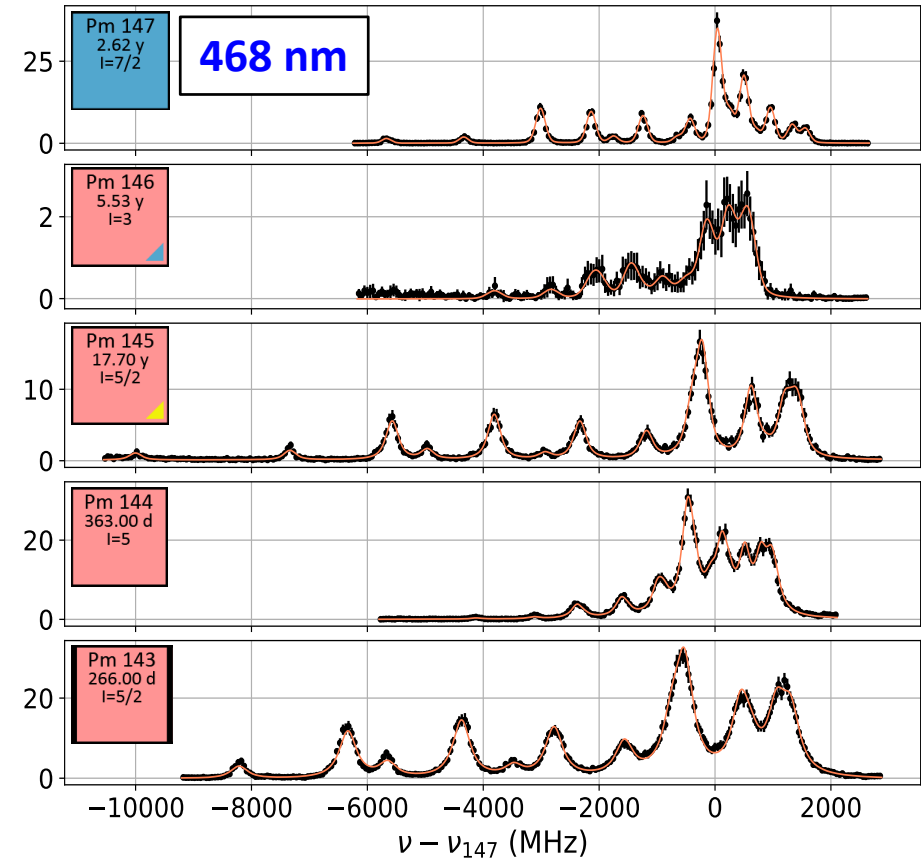
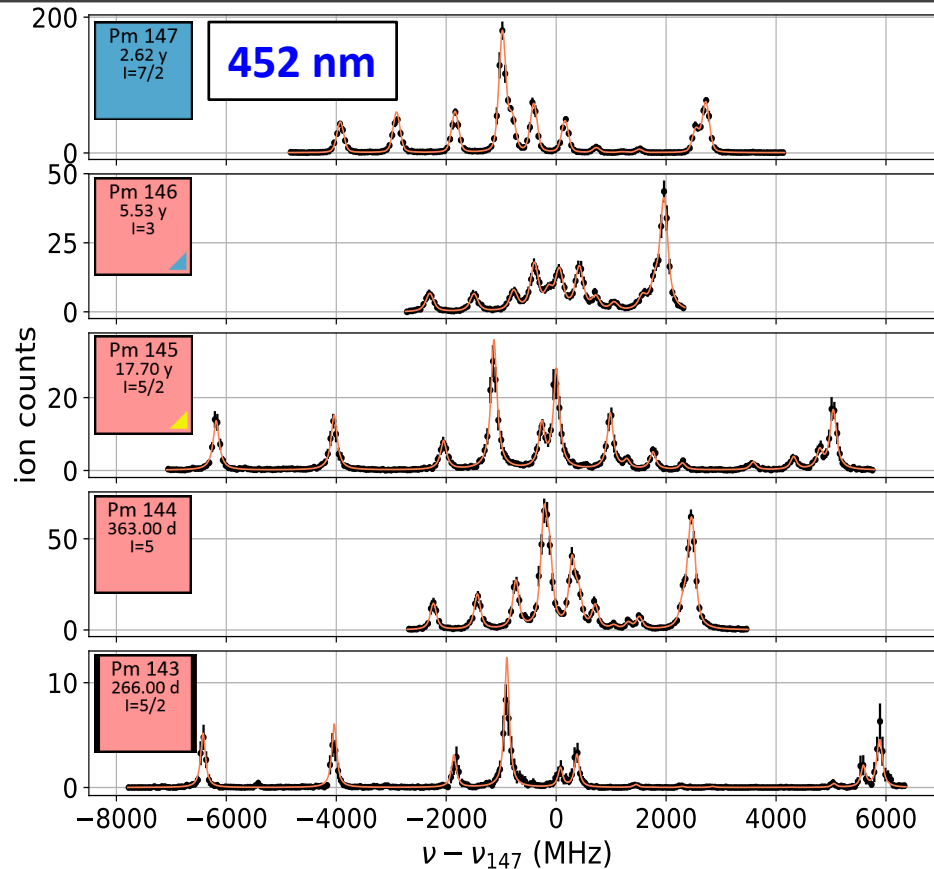


$^{145,147}\text{Pm (II)}$: G.D. Alkhazov et al., J. Phys. B **25** (1992) 571-576

High Resolution In-Source Laser Spectroscopy



HFS spectra of $^{143-147}\text{Pm}$



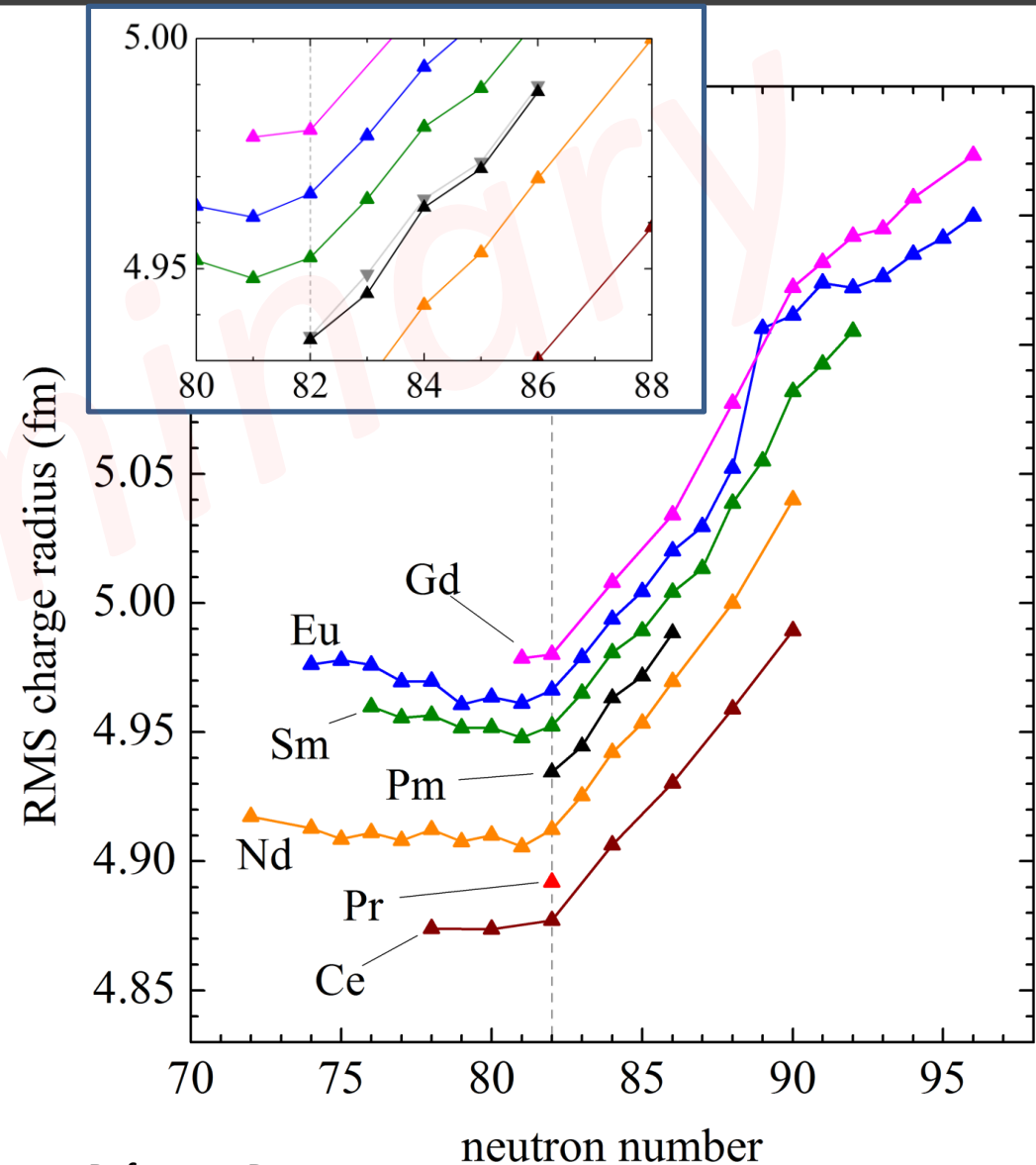
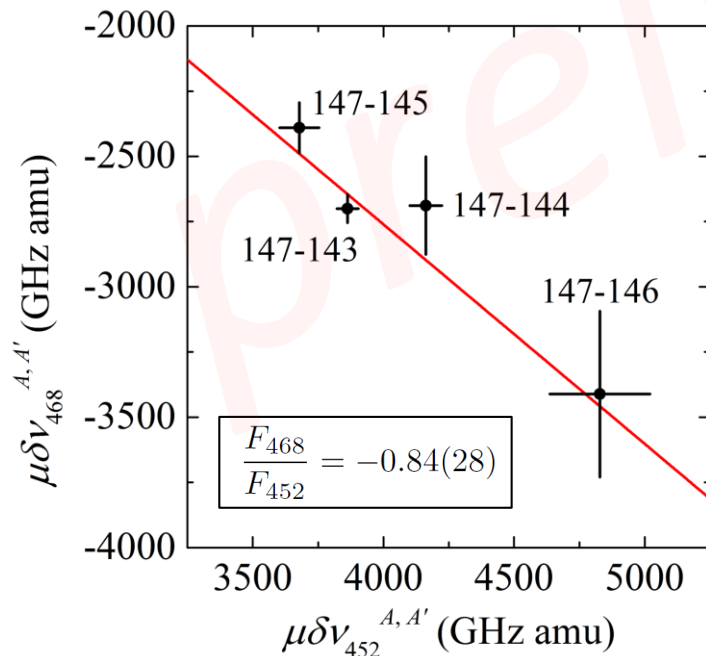
Isotope	$\nu - \nu_{147}$ (MHz)	A_{GS} (MHz)	A_{FES} (MHz)	B_{GS} (MHz)	B_{FES} (MHz)
147	0(6)	619.9(2)	499.6(2)	-409(2)	-119(3)
146	225(6)	429.0(3)	345.7(4)	5(3)	1.5(10)
145	347(5)	1255.5(2)	1011.9(1)	-139(2)	-40(1)
144	596(6)	329.0(2)	265.1(2)	127(3)	37(1)
143	736(7)	1368.8(7)	1103.2(6)	-66(6)	-19(2)

- exp. linewidth FWHM **~100 MHz**
- extracted A and B parameters agree for 452 nm and 468 nm transition

452 nm transition

Nuclear Charge Radii in Pm

- Electronic factor ratio from King-Plot
- SMS** neglected, **F** interpolated from neighboring elements
- Indication of small odd-even staggering



Reference Data:

I. Angeli, K.P. Marinova / Atomic Data and Nuclear Data Tables 99 (2013) 69–95

Conclusion and Outlook

- **High resolution laser spectroscopy** delivers most valuable **nuclear ground state properties** as well as **atomic physics information** within long isotopic chains up to the most exotic, short-lived isotopes
 - Experimental resolution in the order of natural atomic line widths needed
- Collinear Laser Spectroscopy still is the most versatile technique
- Various sensitive detection techniques are in use
 - **Standard fluorescence detection** still very prosperous after 40 years of use
 - **Nuclear polarization** and β -NMR detection
 - **Resonance ionization** enables efficient detection of ions or nuclear decays
 - **Cooler and buncher** combinations for background reduction
 - On-line Collinear **Photodetachment Spectroscopy** for study on exotic negative ions
- **Alternative techniques** found in high resolution **in-source** spectroscopy

Acknowledgements



Thank you for your attention – and these gentlemen and their actual colleagues for their work

Ultra Trace Analysis by Collinear Fast Beam Laser Spectroscopy

$^{89,90}\text{Sr}$ Ultra Trace Analysis by RIMS

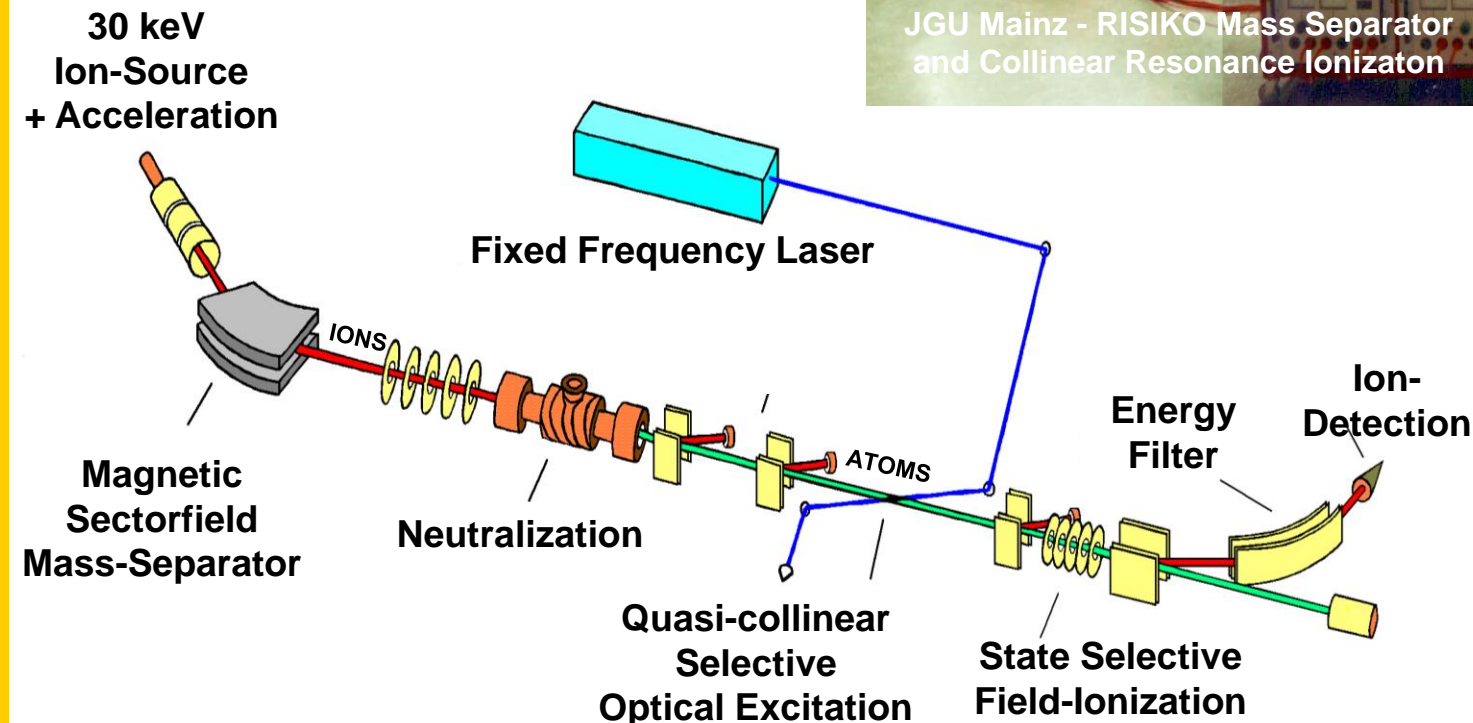
Isotopic Selectivity: $\geq 10^{10}$
(background limited)

Overall Efficiency : $\sim 10^{-5}$
(laserpower limited)

Detection Limit : $\sim 3 \times 10^6$ atoms ^{90}Sr
per sample (~ 2 mBq)



JGU Mainz - RISIKO Mass Separator
and Collinear Resonance Ionization

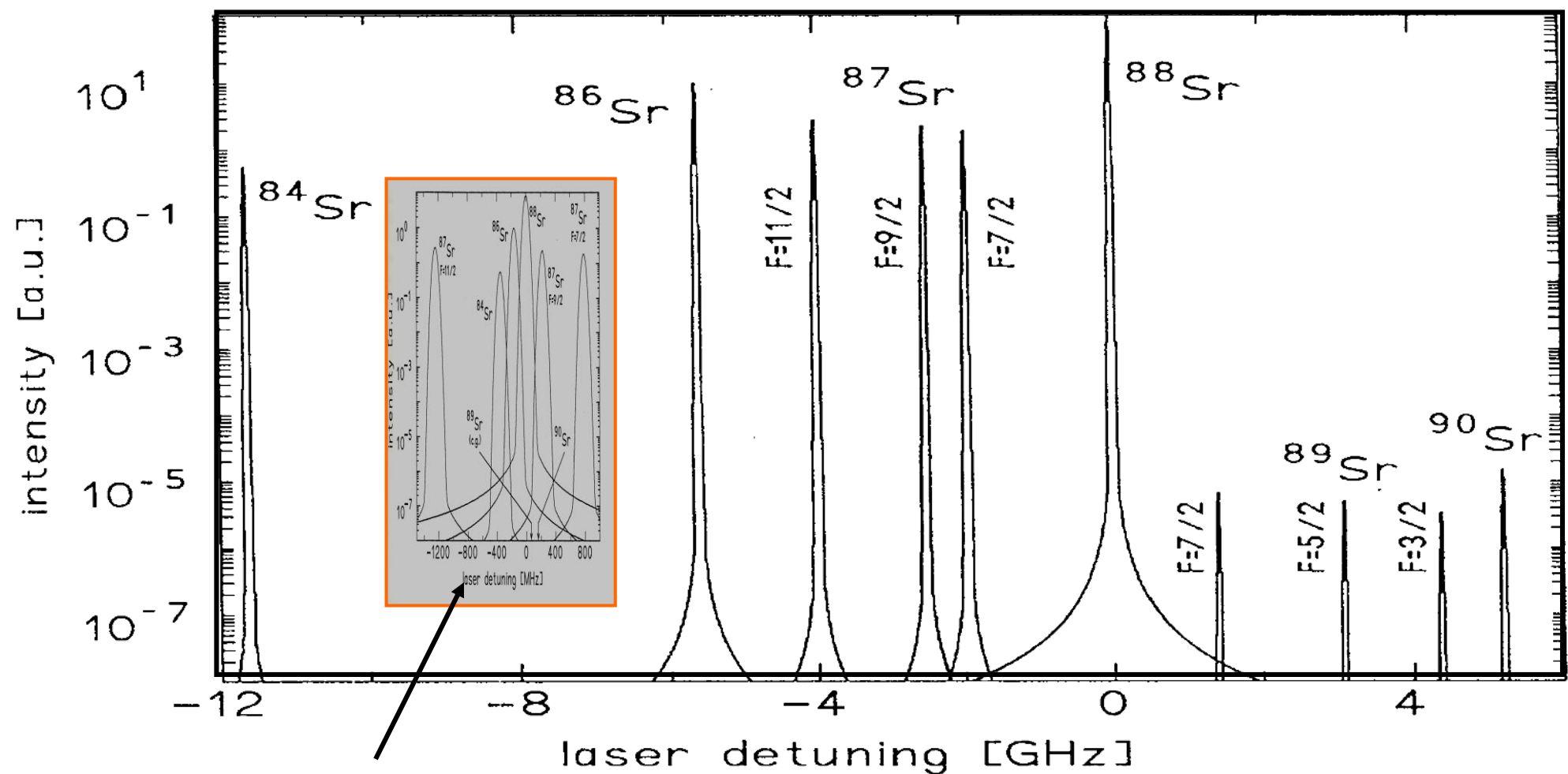


1-Step Quasi-collinear RIS

$5s\ 4d\ ^3D_J \rightarrow 5s\ 23f\ ^3F_J$
(363.8 nm)

+
17 keV field ionization

Isotope Selection by Collinear Fast Beam Laser Spectroscopy



No isotope resolution - no selectivity

Fast atomic beam (energy 50 keV):
Selectivity $> 10^9$ per excitation step